
Addressing Polarization and Unfairness in Performative Prediction

Kun Jin *

University of Michigan, Ann Arbor
kunj@umich.edu

Tian Xie*

the Ohio State University
xie.1379@osu.edu

Yang Liu

University of California, Santa Cruz
yangliu@ucsc.edu

Xueru Zhang

the Ohio State University
zhang.12807@osu.edu

Abstract

When machine learning (ML) models are used in applications that involve humans (e.g., online recommendation, school admission, hiring, lending), the model itself may trigger changes in the distribution of targeted data it aims to predict. *Performative prediction* (PP) is a framework that explicitly considers such model-dependent distribution shifts when learning ML models. While significant efforts have been devoted to finding *performative stable* (PS) solutions in PP for system robustness, their societal implications are less explored and it is unclear whether PS solutions are aligned with social norms such as fairness. In this paper, we set out to examine the fairness property of PS solutions in performative prediction. We first show that PS solutions can incur severe polarization effects and group-wise loss disparity. Although existing fairness mechanisms commonly used in literature can help mitigate unfairness, they may fail and disrupt the stability under model-dependent distribution shifts. We thus propose novel fairness intervention mechanisms that can simultaneously achieve both stability and fairness in PP settings. Both theoretical analysis and experiments are provided to validate the proposed method.

1 Introduction

Modern supervised learning excels in many domains, especially in pattern recognition where the target data distribution is static and independent of the deployed model. However, in the presence of *model-dependent* distribution shifts (i.e., the model itself triggers the changes in the distribution of targeted data), most conventional training approaches will fail to find solutions that are stable and robust to such shifts. In fact, model-dependent distribution shifts are practical and commonly exist in real-world applications. Examples include strategic individuals manipulating their data (in school admission, hiring, or lending) to game the ML system into making favorable predictions [1], consumers changing their retention and participation choices (in digital platforms) based on their perception toward the ML model they are subject to [2, 3], etc.

To make predictions in the presence of model-dependent distribution shifts, Perdomo et al. [4] proposed **performative prediction** (PP), a framework that explicitly considers the target data distribution $\mathcal{D}(\theta)$ as a function of the ML model parameter θ to be optimized. While PP captures the impacts of the ML model on target data, the distribution $\mathcal{D}(\theta)$ is solely determined by the model regardless of the original data distribution. A subsequent study [5] extended PP and proposed a more generalized **state-dependent performative prediction** (SDPP) framework, which considers the impacts of both

*These authors contribute equally.

model and initial data distribution. Specifically, given the deployed ML model parameter θ and initial data distribution \mathcal{D} , SDPP models the resulting target data distribution $\mathcal{D}' = T(\theta; \mathcal{D})$ using some transition mapping function T . Since PP is a special case of SDPP, we focus on SDPP in this paper.

Since the target data distribution depends on the model, the learning objective of SDPP is to minimize **performative risk** (PR), i.e.,

$$\theta^{\text{PO}} = \underset{\theta}{\operatorname{argmin}} \operatorname{PR}(\theta) \stackrel{\text{def}}{=} \mathbb{E}_{Z \sim T(\theta; \mathcal{D})}[\ell(\theta; Z)]$$

where $\ell(\theta; Z)$ is the loss function, Z is the data sampled from the target distribution $T(\theta; \mathcal{D})$ dependant on both model parameter θ to be optimized and the initial data distribution \mathcal{D} . The minimizer θ^{PO} is named as **performative optimal** (PO) solution. Because the target data distribution itself is a function of variable θ to be optimized, finding the PO solution is often challenging [4, 5]. Instead, existing works have mostly focused on finding **performative stable** (PS) solution θ^{PS} , which minimizes the **decoupled performative risk** $\operatorname{DPR}(\theta; \theta^{\text{PS}})$ defined as follows,

$$\theta^{\text{PS}} = \underset{\theta}{\operatorname{argmin}} \operatorname{DPR}(\theta; \theta^{\text{PS}}) \stackrel{\text{def}}{=} \mathbb{E}_{Z \sim T(\theta^{\text{PS}}; \mathcal{D}^{\text{PS}})}[\ell(\theta; Z)] \quad (1)$$

where \mathcal{D}^{PS} is the fixed point data distribution induced by θ^{PS} that satisfies $\mathcal{D}^{\text{PS}} = T(\theta^{\text{PS}}; \mathcal{D}^{\text{PS}})$. Unlike performative risk $\operatorname{PR}(\theta)$ where data distribution $T(\theta; \mathcal{D})$ depends on variable θ to be optimized, decoupled performative risk $\operatorname{DPR}(\theta; \theta^{\text{PS}})$ decouples the two, i.e., data distribution is induced by θ^{PS} while the variable to be optimized is θ . Although in general $\theta^{\text{PS}} \neq \theta^{\text{PO}}$, θ^{PS} is the fixed point of Eqn. (1) and stabilizes the system: at θ^{PS} , data distribution \mathcal{D}^{PS} also remain fixed. Many algorithms have been proposed in the literature to find θ^{PS} . A prime example is *repeated risk minimization* (RRM) [4], an iterative algorithm that finds θ^{PS} (under certain conditions) by repeatedly updating the model $\theta^{(t)}$ that minimizes risk on the fixed distribution $\mathcal{D}^{(t-1)}$ induced by the previous model $\theta^{(t-1)}$, i.e.,

$$\theta^{(t)} = \underset{\theta}{\operatorname{argmin}} \mathbb{E}_{Z \sim \mathcal{D}^{(t-1)}}[\ell(\theta; Z)], \quad \mathcal{D}^{(t)} = T(\theta^{(t)}; \mathcal{D}^{(t-1)}). \quad (2)$$

However, the societal implications of PS solutions are less understood and it is unclear whether PS solutions can cause harm and violate social norms such as fairness.

In this paper, we examine the fairness properties of PS solutions θ^{PS} . We consider scenarios where an ML model is used to make decisions about people from multiple demographic groups, and the population data distribution changes based on the ML decisions they are subject to. We find that PS solutions can 1) incur severe polarization effects: entire population \mathcal{D}^{PS} is dominated by certain groups, leaving the rest marginalized and almost diminished in the sample pool; 2) be biased when deployed on \mathcal{D}^{PS} and people from different groups will experience different losses. However, in many applications such as recommendation systems, school admission, and loan applications, it is critical to ensure equal quality of ML predictions and population diversity. Thus, we investigate under what conditions and by what algorithms we can simultaneously achieve stability and fairness in SDPP.

Focusing on group-wise *loss disparity* [6, 7] and *participation disparity* [2, 8] fairness measures, we first explore whether existing fairness mechanisms commonly used in supervised learning can help mitigate unfairness in SDPP settings; this includes *regularization methods* (adding fairness violation as a penalty term to the objective function of unconstrained optimization, e.g., [9, 10]) and *re-weighting methods* (adjusting weights and importance of samples in learning objective, e.g., [11, 12, 13]). We show that common choices of penalty terms (e.g., group-wise loss difference) and re-weighting designs (e.g., standard distributionally robust optimization) that are effective in traditional supervised learning may fail in SDPP settings by disrupting the stability of the system. Using repeated risk minimization (RRM) shown in Eqn. (2) as an example, this means that applying such fairness mechanisms at each round of RRM can disrupt the convergence of the algorithm and $(\theta^{(t)}, \mathcal{D}^{(t)})$ may diverge to an unexpected state. We thus propose novel fairness mechanisms, which can be easily adopted and incorporated into iterative algorithms such as RRM. We theoretically show that the proposed mechanism can effectively improve fairness while maintaining the stability of the system.

It is worth noting that although a few recent works also studied fairness issues under model-dependent distribution shifts, they all make rather strong assumptions about the distribution shifts and do not

apply to the general SDPP framework. For example, Raab et al. [8], Zezulka and Genin [14], Hu and Zhang [15] assumed there exists a causal model that depicts how data distribution would shift based on the ML model, and these causal models need to be fully known. Raab et al. [8] studied a special type of model-dependent distribution shift where only the group proportion/participation changes based on ML models. In Appendix A, we discuss these works in more detail and provide a comprehensive literature review.

The rest of the paper is organized as follows. Section 2 provides the background of SDPP. Section 3 formulates the problem and demonstrates the unfairness and polarization issues of PS solutions. Section 4 highlights the difficulties of simultaneously achieving fairness and stability in SDPP, where we first show that existing fairness mechanisms commonly used in supervised learning may fail in SDPP settings and then propose a novel fairness mechanism. In Section 5, we conduct the theoretical analysis and show that our method can effectively improve fairness while maintaining stability. Finally, Section 6 empirically validates the proposed method on both synthetic and real data.

2 Preliminaries: Iterative Algorithms to Find PS Solutions in SDPP

As mentioned in Section 1, the original goal of SDPP is to find the performative optimal solution θ^{PO} that minimizes the performative risk $\text{PR}(\theta) = \mathbb{E}_{Z \sim T(\theta; \mathcal{D})}[\ell(\theta; Z)]$, the loss over the population induced by the deployed model. However, solving this optimization is often challenging because the data distribution $T(\theta; \mathcal{D})$ depends on the variable θ to be optimized. Thus, prior studies such as [4, 5] have mostly focused on finding performative stable solution θ^{PS} , which is the fixed point of Eqn. (1) and can be found through an iterative process of *data sampling* and *model deployment*. Specifically, denote $\mathcal{L}(\theta; \mathcal{D}) = \mathbb{E}_{Z \sim \mathcal{D}}[\ell(\theta; Z)]$ and let $(\theta^{(t)}, \mathcal{D}^{(t)})$ be the model parameter and data distribution at round t of the iterative algorithm, then repeatedly updating the model $\theta^{(t)}$ according to Eqn. (3) could lead $(\theta^{(t)}, \mathcal{D}^{(t)})$ converging to PS solution $(\theta^{\text{PS}}, \mathcal{D}^{\text{PS}})$ under certain conditions [4, 5].

$$\theta^{(t)} = \underset{\theta}{\operatorname{argmin}} \mathcal{L}(\theta; \mathcal{D}^{(t-1)}), \quad \mathcal{D}^{(t)} = \operatorname{Tr}(\theta^{(t)}; \mathcal{D}^{(t-1)}). \quad (3)$$

where Tr is not necessarily the same as transition mapping T that drives evolution of data. Depending on how frequently the model is deployed compared to the change of data, Tr can be defined differently based on **repeated deployment schema**. Common examples include:

conventional: $\operatorname{Tr}(\theta^{(t)}; \mathcal{D}^{(t-1)}) = T(\theta^{(t)}; \mathcal{D}^{(t-1)})$

k-delayed: $\operatorname{Tr}(\theta^{(t)}; \mathcal{D}^{(t-1)}) = T^k(\theta^{(t)}; \mathcal{D}^{(t-1)}) = \underbrace{T(\theta^{(t)}; \dots T(\theta^{(t)}; T(\theta^{(t)}; \mathcal{D}^{(t-1)})))}_{k \text{ times}}$

delayed: $\operatorname{Tr}(\theta^{(t)}; \mathcal{D}^{(t-1)}) = T^{\lceil r \rceil + 1}(\theta^{(t)}; \mathcal{D}^{(t-1)})$

where the *repeated risk minimization* (RRM) [4] introduced in Section 1 corresponds to conventional deployment schema. By customizing the time interval between two deployments, we can get variants including *delayed RRM* and *k-delayed RRM* [5]. Note that the delayed deployment schema is a special case of k -delayed deployment schema, where the number of repeated deployments r is chosen to ensure the output distribution $\mathcal{D}^{(t)}$ is sufficiently close to the fixed point distribution when $\theta^{(t)}$ keeps being deployed on the population $\mathcal{D}^{(t-1)}$.

Technical conditions for iterative algorithms to converge to PS solutions. As shown in [4, 5], PS solutions exist and are unique only when ℓ and T satisfy certain requirements. Moreover, iterative algorithms introduced in Eqn. (3) can converge to the PS solution. We introduce them below, where Θ , \mathcal{Z} , and $\Delta(\mathcal{Z})$ denote the parameter space, sample space, and space of distributions over samples.

Definition 2.1 (Strong convexity of loss). $\ell(\theta; Z)$ is γ -strongly convex if and only if for all $\theta, \theta' \in \Theta$ and $Z \in \mathcal{Z}$, we have

$$\ell(\theta; Z) \geq \ell(\theta'; Z) + \langle \nabla_{\theta} \ell(\theta; Z), \theta - \theta' \rangle + \frac{\gamma}{2} \|\theta - \theta'\|_2^2.$$

Definition 2.2 (Joint smoothness of loss). $\ell(\theta; Z)$ is β -jointly smooth if the gradient with respect to θ is β -Lipschitz in θ and Z , i.e., $\forall \theta, \theta' \in \Theta$ and $\forall Z, Z' \in \mathcal{Z}$, we have

$$\|\nabla_{\theta} \ell(\theta; Z) - \nabla_{\theta} \ell(\theta'; Z)\|_2 \leq \beta \|\theta - \theta'\|_2, \quad \|\nabla_{\theta} \ell(\theta; Z) - \nabla_{\theta} \ell(\theta; Z')\|_2 \leq \beta \|Z - Z'\|_2.$$

Definition 2.3 (Joint sensitivity of transition). Let \mathcal{W}_1 denote the Wasserstein-1 distance measure. The transition mapping T is ϵ -jointly sensitive if for all $\theta, \theta' \in \Theta$ and $\mathcal{D}, \mathcal{D}' \in \Delta(\mathcal{Z})$,

$$\mathcal{W}_1(T(\theta; \mathcal{D}), T(\theta'; \mathcal{D})) \leq \epsilon \|\theta - \theta'\|_2, \quad \mathcal{W}_1(T(\theta; \mathcal{D}), T(\theta; \mathcal{D}')) \leq \epsilon \mathcal{W}_1(\mathcal{D}, \mathcal{D}').$$

Lemma 2.4 (The existence of a unique PS solution [4, 5]). *The SDPP problem is guaranteed to have a unique PS solution if all of the following hold: (i) Loss $\ell(\theta; Z)$ is γ -strongly convex; (ii) Loss $\ell(\theta; Z)$ is β -joint smooth; (iii) T is ϵ -joint sensitive and $\epsilon(1 + \beta/\gamma) < 1$. Moreover, if any of these conditions is violated, the iterative algorithms may fail to converge to the PS solution.*

3 Unfairness and Polarization in SDPP

Problem Formulation. In this work, we study SDPP with different demographic groups, where an ML model θ is trained to make predictions about individuals from multiple groups distinguished by a sensitive attribute $s \in \mathcal{S}$ (e.g., gender, age, race), whose data distribution changes based on the deployed ML model and such model-dependent distribution shift can be captured by transition mapping T . Suppose individuals from group s follow the identical data distribution $\mathcal{D}_s^{(t)}$ at the round t of an iterative algorithm, and let $p_s^{(t)}$ be the size of group s as the fraction of entire population at t . Then the data distribution of the entire population is $\mathcal{D}^{(t)} = \sum_{s \in \mathcal{S}} p_s^{(t)} \mathcal{D}_s^{(t)}$ with $\sum_{s \in \mathcal{S}} p_s^{(t)} = 1$.

Note that the above SDPP with multiple groups is a general framework. By specifying the transition mapping T , many problems studied in prior works can be regarded as a special case. This includes:

1. **Strategic classification with multiple groups** [16, 17]: individuals in applications such as lending, hiring, and admission may manipulate their data based on ML model strategically to increase their chances of receiving favorable decisions, leading to changes in group distribution $\mathcal{D}_s^{(t)}$.
2. **Decision-making systems under user retention dynamics** [2, 12, 18]: ML models used in recognition or recommendation systems may attract more users if they experience high accuracy but drive away those with less satisfaction, which may cause group proportion $p_s^{(t)}$ to change.

In this paper, we first explore the fairness properties of PS solutions in SDPP, i.e., examining whether θ^{PS} in Eqn. (1) have disparate impacts on different demographic groups. Specifically, we consider two fairness metrics: group-wise *loss disparity* $\Delta_{\mathcal{L}}^{(t)}$ [6, 19] and *participation disparity* $\Delta_p^{(t)}$ [8] measuring the difference of loss $\mathcal{L}(\theta; \mathcal{D}_s^{(t)})$ and fraction $p_s^{(t)}$ across different groups at round t of an iterative algorithm. In examples with two groups $\mathcal{S} = \{a, b\}$, the unfairness can be quantified as

$$\Delta_{\mathcal{L}}^{(t)} := \left| \mathcal{L}(\theta^{(t)}; \mathcal{D}_a^{(t)}) - \mathcal{L}(\theta^{(t)}; \mathcal{D}_b^{(t)}) \right|, \quad \Delta_p^{(t)} := \left| p_a^{(t)} - p_b^{(t)} \right|. \quad (4)$$

Unfairness & polarization effects in SDPP.

We first show (through two toy examples) that PS solutions θ^{PS} in SDPP may have disparate impacts on different groups. Specifically, when finding θ^{PS} using iterative algorithms introduced in Section 2, the process may incur severe *polarization effects* and exhibit unfairness, i.e., certain groups may get marginalized and diminish from the system, and group-wise loss disparity gets exacerbated during the iterative process.

Example 3.1 (Polarization effects of θ^{PS}). *Consider individuals from two groups a, b whose participation in an ML system depends on their perceived loss, i.e., group fraction $p_s^{(t)}$ changes based on the deployed ML model. Suppose individuals from group a and b have fixed data $Z = z_a = 1$ and $Z = z_b = 0$, respectively. Their initial group fractions are $p_a^{(0)} = 0.7, p_b^{(0)} = 0.3$. Consider conventional RRM with mean squared error $\mathcal{L}(\theta; \mathcal{D}^{(t)}) = \sum_{s \in \{a, b\}} p_s^{(t)} (\theta - z_s)^2$ and transition T that satisfies $p_a^{(t+1)} = p_a^{(t)} + 0.1 \cdot [\mathcal{L}(\theta^{(t)}; \mathcal{D}_b^{(t)}) - \mathcal{L}(\theta^{(t)}; \mathcal{D}_a^{(t)})]$, $p_b^{(t+1)} = 1 - p_a^{(t+1)}$ (i.e., group fraction decreases if the group has higher loss). It is easy to see that $p_a^{(t)}$ (resp. $p_b^{(t)}$) monotonically increases (resp. decreases) in t , and the PS solution solely contains people from group a (see Fig. 1).*

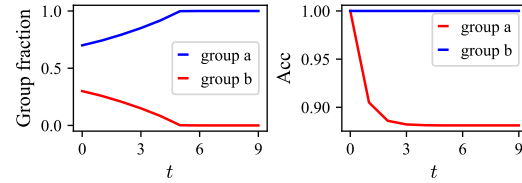


Figure 1: Dynamics of the group fraction in Example 3.1 (left) and group-wise accuracy in Example 3.2 (right) under RRM: the system converges to PS solution ($\theta^{\text{PS}}; \mathcal{D}^{\text{PS}}$) that is unfair.

Example 3.2 (Exacerbated group-wise loss disparity). Consider individuals from two groups a, b who are subject to certain ML decisions; each has an initial feature $X \sim \text{Uniform}(0, 1)$ and a binary label $Y = \mathbb{1}(X \geq 0.5) \in \{0, 1\}$. Suppose the population has fixed group fractions $p_a = 0.7, p_b = 0.3$, but individuals may strategically manipulate their features to increase their chances of receiving favorable ML decisions, i.e., distribution of each group $\mathcal{D}_s^{(t)}$ changes based on ML model. Following the individual response model in [16, 20], we suppose individuals from two groups have certain effort budgets $\eta_a = 0.2, \eta_b = 0.01$ that can be used to improve their features $X_s^{(t+1)} = X_s^{(t)} + \eta_s \cdot \theta^{(t)}$. Consider RRM iterative algorithm where the model parameter $\theta^{(t)}$ is updated to maximize prediction accuracy $\Pr(\mathbb{1}(X \geq \theta^{(t)}) = Y^{(t)})$. Given an initial model $\theta^{(0)} = 0.5$, it is trivial to see that $\theta^{(t)}$ increases over time to be robust against manipulation until converges to PS solution $\theta^{PS} = 0.625$ (see Fig. 1). However, at the PS solution, the accuracy for group a is 1 but is only 0.88 for group b .

4 Fair-PS Solutions and Fairness Mechanisms

Section 3 shows that without fairness consideration, PS solution of SDPP may incur polarization effects and have disparate impacts on different groups, i.e., when finding θ^{PS} using iterative algorithms such as RRM, group-wise loss disparity $\Delta_{\mathcal{L}}^{(t)}$ and participation disparity $\Delta_p^{(t)}$ may get exacerbated and converge to an unfair state. In this section, we address unfairness issues in SDPP. One straightforward idea is to directly apply the fairness mechanisms at every round of the iterative algorithms introduced in Section 2. However, we will show that although such methods are effective in conventional supervised learning, they can disrupt the stability and the iterative algorithms may no longer converge.

4.1 Fairness mechanisms and Fair-PS solutions

Many fairness mechanisms have been proposed in supervised learning to mitigate group-wise loss disparity and participation disparity. We consider two categories commonly used in the literature: *regularization method* and *sample re-weighting method*, as detailed below.

1. **Fairness via regularization:** It adds a regularization/penalty term to the original learning objective function $\mathcal{L}(\theta; \mathcal{D})$, which penalizes the violation of fairness [9, 10]. The fair objective function is

$$\mathcal{L}_{\text{fair}}(\theta; \mathcal{D}, \rho) := \mathcal{L}(\theta; \mathcal{D}) + \mathcal{P}(\theta; \mathcal{D}, \rho), \quad (5)$$

where $\mathcal{P}(\theta; \mathcal{D}, \rho)$ is the fair penalty term and the scalar $\rho > 0$ controls the strength of the penalty.

2. **Fairness via sample re-weighting:** It adjusts the weights of samples (possibly adversarially) and increases sample weights for disadvantaged groups [11, 12, 13]. One example is distributionally robust optimization (DRO) [18], which minimizes the worst-case loss and the fair objective is

$$\mathcal{L}_{\text{fair}}(\theta; \mathcal{D}, \rho) := \max_{\tilde{\mathcal{D}} \in \mathcal{B}(\mathcal{D}, r(\rho))} \mathcal{L}(\theta; \tilde{\mathcal{D}}), \quad (6)$$

where $\mathcal{B}(\mathcal{D}, r(\rho)) := \{\tilde{\mathcal{D}} | d(\mathcal{D}, \tilde{\mathcal{D}}) \leq r(\rho)\}$ denotes a distribution ball centered at \mathcal{D} with radius $r(\rho)$ derived from the fair mechanism strength ρ , and d is a distribution distance metric.

By optimizing a fair objective $\mathcal{L}_{\text{fair}}(\theta; \mathcal{D}, \rho)$, existing fairness mechanisms can effectively mitigate unfairness in supervised learning with static data distribution \mathcal{D} . However, it remains unclear how these methods would perform in SDPP when the model itself causes the data distribution shifts. Specifically, consider iterative algorithms introduced in Eqn. (3) that find PS solutions (e.g., RRM). Suppose we apply the above fairness mechanism at every round when updating the model parameter θ , i.e., replacing $\theta^{(t)} = \text{argmin}_{\theta} \mathcal{L}(\theta; \mathcal{D}^{(t-1)})$ with fair version $\theta^{(t)} = \text{argmin}_{\theta} \mathcal{L}_{\text{fair}}(\theta; \mathcal{D}^{(t-1)}, \rho)$ in iterative algorithms. We ask: *can such new iterative algorithms mitigate group-wise loss and participation disparity in SDPP and converge to a fair and stable solution?*

Before answering the above question, we first define **Fair-PS solutions** for SDPP, at which both ML system and population distribution reach stability and unfairness is mitigated.

Definition 4.1 (Fair-PS solution). We define $(\mathcal{D}_{\text{fair}}^{\text{PS}}, \theta_{\text{fair}}^{\text{PS}})$ as the Fair-PS solution to $\mathcal{L}_{\text{fair}}(\theta; \mathcal{D}, \rho)$ if

$$\mathcal{D}_{\text{fair}}^{\text{PS}} = \text{T}(\theta_{\text{fair}}^{\text{PS}}; \mathcal{D}_{\text{fair}}^{\text{PS}}), \quad \theta_{\text{fair}}^{\text{PS}} = \text{argmin}_{\theta} \mathcal{L}_{\text{fair}}(\theta; \mathcal{D}_{\text{fair}}^{\text{PS}}, \rho).$$

4.2 Existing designs fail to converge to Fair-PS solutions

We will use two examples to illustrate that the popular choices of fairness mechanisms used in previous literature may fail to achieve stability and fairness in SDPP. This includes (i) regularization method [9, 10] with *group loss variance* $\mathcal{P}(\boldsymbol{\theta}; \mathcal{D}, \rho) := \rho \sum_{s \in \mathcal{S}} p_s \cdot [\mathcal{L}(\boldsymbol{\theta}; \mathcal{D}_s) - \mathcal{L}(\boldsymbol{\theta}; \mathcal{D})]^2$ as the penalty term in Eqn. (5); and (ii) *distributionally robust optimization* (DRO) method [19, 21] with χ^2 -distance metric $d(\mathcal{D}, \tilde{\mathcal{D}}) := \int \left(\frac{d\tilde{\mathcal{D}}}{d\mathcal{D}} - 1 \right)^2 d\tilde{\mathcal{D}}$ in Eqn. (6).

Example 4.2 (Group loss variance as penalty term). *Consider two groups a, b with data $Z = (X, Y)$ and fixed group fractions $p_a = p_b = 0.5$. Suppose all samples in group a are $(1, -1)$ and all samples in group b are $(2, 1)$. Consider squared loss function $\ell(z; \theta) = (y - h_\theta(x))^2 = (y - \theta x)^2$ which is strongly convex and jointly smooth. Under group loss variance penalty $\mathcal{P}(\boldsymbol{\theta}; \mathcal{D}, \rho)$, we have $\mathcal{L}_{\text{fair}}(\boldsymbol{\theta}; \mathcal{D}, \rho) = 2.5\theta^2 - \theta + 1 + \rho \cdot (2.25\theta^4 + 9\theta^2 - 9\theta^3)$. When $\rho = 0.6$, the second-order derivative $\nabla_\theta^2 \mathcal{L}_{\text{fair}} = 16.2\theta^2 - 32.4\theta + 15.8$ and is negative when $\theta = 1$. Because convexity of $\mathcal{L}_{\text{fair}}$ is a **necessary** condition for iterative algorithms such as RRM to converge to a stable solution (by Lemma 2.4), adding group loss variance as a penalty at each round will disrupt the stability and the algorithm fails to find Fair-PS solutions. Appendix C.4 provides an empirical illustration of this.*

Example 4.3 (Repeated DRO with χ^2 -distance metric). *Consider two groups a, b with fixed data $z_a = 1$ and $z_b = -1$ for all samples but group fractions $p_a^{(t)} = 0.5 \cdot (1 + \theta^{(t)})$ and $p_b^{(t)} = 0.5 \cdot (1 - \theta^{(t)})$. $p_a^{(0)} = 0.4, p_b^{(0)} = 0.6$. Consider a mean estimation task where the model parameter $\theta^{(t+1)} := \arg \min_{\theta} \max_{\tilde{\mathcal{D}} \in \mathcal{B}(\mathcal{D}^{(t)}, r)} \mathcal{L}(\theta; \tilde{\mathcal{D}})$ is updated using DRO with mean squared error and χ^2 -distance bound $r = 1/6$. Let $q_a^{(t)}, q_b^{(t)}$ denote the group fractions of "worst-case" distribution $\tilde{\mathcal{D}}$. We have $q_a^{(0)} = 0.6, q_b^{(0)} = 0.4$ and $\theta^{(1)} = \arg \min_{\theta} q_a^{(0)}(1 - \theta)^2 + q_b^{(0)}(1 + \theta)^2 = 0.2$, which results in $p_a^{(1)} = 0.6, p_b^{(1)} = 0.4$. Since $\mathcal{L}_a(\theta^{(1)}; z_a) < \mathcal{L}_b(\theta^{(1)}; z_b)$, DRO should minimize the risk of the "worst-case" distribution with $q_a^{(1)} = 0.4, q_b^{(1)} = 0.6$, i.e., $\theta^{(2)} = \arg \min_{\theta} q_a^{(1)}(1 - \theta)^2 + q_b^{(1)}(1 + \theta)^2 = -0.2$. Repeating the procedure we will get $p_a^{(2)} = 0.4, p_b^{(2)} = 0.6$ and $q_a^{(2)} = 0.6, q_b^{(2)} = 0.4, \theta^{(3)} = 0.2$. It turns out that repeated DRO results in $\theta^{(t)}$ oscillating between 0.2 and -0.2 and it never converges.*

It is worth noting that DRO methods have been used in Hashimoto et al. [19] to mitigate group fraction disparity in repeated optimizations. However, it only improves fairness without any convergence guarantees to stable solutions. Peet-Pare et al. [21] repeatedly used DRO to improve fairness under PP settings, it only converges to a PS solution under strict assumptions that are hard to verify. Under milder conditions in Lemma 2.4, it may fail to converge as Example 4.3 illustrated.

4.3 Novel designs for fairness mechanism

Next, we introduce three novel fair objective functions $\mathcal{L}_{\text{fair}}(\boldsymbol{\theta}; \mathcal{D}, \rho)$ for fairness mechanisms, of which two belong to *regularization method* and one is a *sample re-weighting method*. By replacing $\boldsymbol{\theta}^{(t)} = \arg \min_{\boldsymbol{\theta}} \mathcal{L}(\boldsymbol{\theta}; \mathcal{D}^{(t-1)})$ with the proposed fair update $\boldsymbol{\theta}^{(t)} = \arg \min_{\boldsymbol{\theta}} \mathcal{L}_{\text{fair}}(\boldsymbol{\theta}; \mathcal{D}^{(t-1)}, \rho)$ in Eqn. (3), the resulting iterative algorithms can converge to Fair-PS solutions.

Proposed fair regularization (with and without demographics). Depending on whether sensitive attributes S are accessible during training, we propose two fairness penalty terms, as detailed below.

1. **Group level fairness penalty:** It updates model parameter $\boldsymbol{\theta}^{(t)}$ at round t by the following

$$\boldsymbol{\theta}^{(t)} = \arg \min_{\boldsymbol{\theta}} \mathcal{L}_{\text{fair}}(\boldsymbol{\theta}; \mathcal{D}^{(t-1)}, \rho) := \mathcal{L}(\boldsymbol{\theta}; \mathcal{D}^{(t-1)}) + \rho \sum_{s \in \mathcal{S}} p_s^{(t-1)} [\mathcal{L}(\boldsymbol{\theta}; \mathcal{D}_s^{(t-1)})]^2 \quad (7)$$

2. **Sample level fairness penalty without demographics:** It updates model parameter $\boldsymbol{\theta}^{(t)}$ at round t as follows, which does not need the knowledge of sensitive attributes.

$$\boldsymbol{\theta}^{(t)} = \arg \min_{\boldsymbol{\theta}} \mathcal{L}_{\text{fair}}(\boldsymbol{\theta}; \mathcal{D}^{(t-1)}, \rho) := \mathcal{L}(\boldsymbol{\theta}; \mathcal{D}^{(t-1)}) + \rho \mathbb{E}_{Z \sim \mathcal{D}^{(t-1)}} [[\ell(\boldsymbol{\theta}; Z)]^2]. \quad (8)$$

Proposed fair sample re-weighting. It updates model parameter $\boldsymbol{\theta}^{(t)}$ at round t as follows.

$$\boldsymbol{\theta}^{(t)} = \arg \min_{\boldsymbol{\theta}} \mathcal{L}_{\text{fair}}(\boldsymbol{\theta}; \mathcal{D}^{(t-1)}, \rho) := \sum_{s \in \mathcal{S}} q_s^{(t-1)} \mathcal{L}(\boldsymbol{\theta}; \mathcal{D}_s^{(t-1)}), \quad (9)$$

with $\mathbf{q}^{(t-1)} = \left[q_s^{(t-1)} \right]_{s \in \mathcal{S}} := \frac{\mathbf{p}^{(t-1)} + \rho \mathbf{l}^{(t-1)}}{\|\mathbf{p}^{(t-1)} + \rho \mathbf{l}^{(t-1)}\|_1}$ and $\mathbf{l}^{(t-1)} := \left[p_s^{(t-1)} \mathcal{L}(\boldsymbol{\theta}^{(t-1)}; \mathcal{D}_s^{(t-2)}) \right]_{s \in \mathcal{S}}$

Unlike DRO methods in [19, 22] that require solving a min-max optimization at the current round, our re-weighting method only adjusts the weights for each group based on the group-wise losses in the previous round, which is more computationally efficient.

Comparison & discussion. Intuitively, compared to original $\mathcal{L}(\boldsymbol{\theta}; \mathcal{D}^{(t-1)})$, all three proposed fair objective functions $\mathcal{L}_{\text{fair}}(\boldsymbol{\theta}; \mathcal{D}^{(t-1)}, \rho)$ improves fairness at each round by assigning more weights to disadvantaged groups/samples (i.e., the groups/samples experiencing higher losses) in the upcoming update. Indeed, both *sample level fairness penalty* and *fair sample re-weighting* can be regarded as modifications of *group level fairness penalty*.

Comparing Eqn. (7) and (8), the two penalty terms get more similar when most individual samples in the disadvantaged (resp. advantaged) groups are also similarly disadvantaged (resp. advantaged). This is more likely to happen when each demographic group has a distribution with a small variance. For example, if the distribution of each group is a point mass, Eqn. (7) and (8) are identical.

Comparing Eqn. (7) and (9), we can rewrite Eqn. (9) as the following:

$$\|\mathbf{p}^{(t-1)} + \rho \mathbf{l}^{(t-1)}\|_1 \mathcal{L}_{\text{fair}}(\boldsymbol{\theta}; \mathcal{D}^{(t-1)}, \rho) = \sum_{s \in \mathcal{S}} p_s^{(t-1)} (1 + \rho) \mathcal{L}(\boldsymbol{\theta}^{(t-1)}; \mathcal{D}_s^{(t-2)}) \mathcal{L}(\boldsymbol{\theta}; \mathcal{D}_s^{(t-1)}).$$

We can see that the right-hand side will be a multiple of Eqn. (7) if we replace $\mathcal{L}(\boldsymbol{\theta}^{(t-1)}; \mathcal{D}_s^{(t-2)})$ with $\mathcal{L}(\boldsymbol{\theta}; \mathcal{D}_s^{(t-1)})$. This means both equations yield the same $\boldsymbol{\theta}^{(t)}$ when the population distribution does not change from $t-2$ to $t-1$, suggesting that the two approaches become more similar when the sensitivity of the transition mapping T is smaller, or equivalently, the distribution shift is milder. Finally, we also discuss designing fair objective functions generally in App. B.4.

5 Theoretical Analysis

Next, we show that by replacing update $\boldsymbol{\theta}^{(t)} = \operatorname{argmin}_{\boldsymbol{\theta}} \mathcal{L}(\boldsymbol{\theta}; \mathcal{D}^{(t-1)})$ in Eqn. (3) with the fair update $\boldsymbol{\theta}^{(t)} = \operatorname{argmin}_{\boldsymbol{\theta}} \mathcal{L}_{\text{fair}}(\boldsymbol{\theta}; \mathcal{D}^{(t-1)}, \rho)$ we proposed in Section 4.3, Fair-PS solutions (Definition 4.1) exist under certain conditions and the resulting iterative algorithms (see Algorithm 1) can converge to such Fair-PS solutions. We assume conditions in Lemma 2.4 hold in this section and there exists a unique PS solution in the original SDPP problem.

Algorithm 1 Fair repeated risk minimization (Fair-RRM)

Input: $t = 0$, initial data distribution $\mathcal{D}^{(0)}$, strength of fair mechanism ρ , initial model parameter $\boldsymbol{\theta}^{(0)}$, stopping criteria τ
Choose repeated deployment schema and fair mechanism;
repeat
 $\boldsymbol{\theta}^{(t+1)} \leftarrow \operatorname{argmin}_{\boldsymbol{\theta}} \mathcal{L}_{\text{fair}}(\boldsymbol{\theta}; \mathcal{D}^{(t)}, \rho);$
Get $\mathcal{D}^{(t+1)} = \operatorname{Tr}(\boldsymbol{\theta}^{(t+1)}; \mathcal{D}^{(t)})$ from the chosen schema;
 $t \leftarrow t + 1;$
until $\|\boldsymbol{\theta}^{(t)} - \boldsymbol{\theta}^{(t-1)}\|_2 \leq \tau$

We first define a parameter $\tilde{\beta}$ which will be frequently used in the theorems introduced below.

$$\tilde{\beta} := \begin{cases} (2\rho\bar{\ell} + 1)\beta, & \text{for fair regularization method with group level (7) or sample level penalty (8)} \\ (\rho\bar{\ell} + 1)\beta, & \text{for fair sample re-weighting method (9)} \end{cases}$$

where $\bar{\ell} := \sup_{\boldsymbol{\theta}, Z} \ell(\boldsymbol{\theta}; Z)$. We can identify conditions under which a unique Fair-PS solution exists.

Proposition 5.1 (Existence of unique Fair-PS solution). *For a given population with initial distribution $\mathcal{D}^{(0)}$ and the proposed fair mechanism $\mathcal{L}_{\text{fair}}$ with strength ρ , there is a unique Fair-PS solution if $\epsilon(1 + \tilde{\beta}/\gamma) < 1$. Moreover, $(\mathcal{D}_{\text{fair}}^{\text{PS}}, \boldsymbol{\theta}_{\text{fair}}^{\text{PS}})$ is independent of the choice of repeated deployment schema.*

Although the choice of repeated deployment schema does not affect the Fair-PS solution $(\mathcal{D}_{\text{fair}}^{\text{PS}}, \boldsymbol{\theta}_{\text{fair}}^{\text{PS}})$, it influences the convergence rate of the iterative algorithms as stated in Theorem 5.2.

Theorem 5.2 (Convergence of Fair-RRM). *Under **conventional deployment schema**, Algorithm 1 converges to the Fair-PS solution at a linear rate if $\epsilon(1 + \tilde{\beta}/\gamma) < 1$; under **k-delayed deployment schema**, Algorithm 1 converges to the Fair-PS solution at a linear rate for any k if $\epsilon(1 + \tilde{\beta}/\gamma) < 1 - \epsilon$; Particularly, under **delayed deployment schema** when $r = \log^{-1}(\frac{1}{\epsilon}) \log\left(\frac{\mathcal{W}_1(\mathcal{D}^{(0)}, \mathcal{D}^{(1)})}{\delta}\right)$, Algorithm 1 converges to a radius δ of the Fair-PS solution (i.e., $\|\boldsymbol{\theta}^{(t)} - \boldsymbol{\theta}_{\text{fair}}^{\text{PS}}\|_2 \leq \delta$ and $\mathcal{W}_1(\mathcal{D}(\boldsymbol{\theta}^{(t)}), \mathcal{D}_{\text{fair}}^{\text{PS}}) \leq \delta$) in $\mathcal{O}(\log^2 \frac{1}{\delta})$ steps if $\epsilon(1 + \tilde{\beta}/\gamma) < 1$.*

In Appendix B.3, we extend the Algorithm 1 to practical scenarios when data distribution is inaccessible. We provide the algorithm *fair repeated empirical risk minimization (Fair-RERM)* where only limited data samples are available from $\mathcal{D}^{(t)}$ and analyze its sample complexity in Theorem B.3.

Impacts of strength of fair mechanism ρ . Theorem 5.2 and B.3 show that repeatedly minimizing $\mathcal{L}_{\text{fair}}(\theta; \mathcal{D}^{(t-1)}, \rho)$ on evolving data sequence can lead the system converging to a Fair-PS solution. Note that ρ controls the strength of fairness and different ρ could result in different $(\theta_{\text{fair}}^{\text{PS}}, \mathcal{D}_{\text{fair}}^{\text{PS}})$. In conventional supervised learning with static data distribution \mathcal{D} , it is trivial to see that larger ρ in $\mathcal{L}_{\text{fair}}(\theta; \mathcal{D}, \rho)$ will lead to a fairer solution [6]. However, in SDPP with model-dependent distribution shifts, the impact of ρ on unfairness is less straightforward. Because both data distribution $\mathcal{D}_{\text{fair}}^{\text{PS}}$ and model $\theta_{\text{fair}}^{\text{PS}}$ depend on ρ , analyzing how group-wise disparity would change as ρ varies can be highly non-trivial and has not been studied in PP literature (Appendix D.4 provides more discussion).

Next, we initiate the study for fair mechanism in Eqn. (7) with *group-level fairness penalty* and rigorously show that the larger ρ can lead to smaller group-wise loss disparity at the Fair-PS solution. We will focus on a special case of user retention dynamics [2, 19] with two groups $s \in \{a, b\}$, where the group distribution \mathcal{D}_s is fixed but the fraction $p_s^{(t)}$ changes based on group loss $\mathcal{L}(\theta^{(t)}; \mathcal{D}_s)$ during repeated risk minimization process.

Assumption 5.3. At each round, the group that is majority also experiences lower expected loss, i.e., $\arg \max_{s \in \{a, b\}} p_s^t = \arg \min_{s \in \{a, b\}} \mathcal{L}(\theta^{(t)}; \mathcal{D}_s)$. Moreover, for any two models deployed on population $\mathcal{D}^{(t)}$, the model with larger loss disparity $\Delta_{\mathcal{L}}^{(t)}$ leads to higher group fraction disparity $\Delta_p^{(t+1)}$ at time $t + 1$.

Assumption 5.3 is natural: in fields such as recognition or recommendation systems, the minority group contributing less training data suffers from higher loss and has a lower retention rate.

Theorem 5.4 (Larger ρ leads to stronger fairness). *Denote Fair-PS solution $(\theta_{\text{fair}}^{\text{PS}}(\rho), \mathcal{D}_{\text{fair}}^{\text{PS}}(\rho))$ as a function of $\rho \geq 0$. Let $\Delta_{\text{fair}, \mathcal{L}}^{\text{PS}}(\rho)$ be the group-wise loss disparity of $\theta_{\text{fair}}^{\text{PS}}(\rho)$ evaluated over distribution $\mathcal{D}_{\text{fair}}^{\text{PS}}(\rho)$ as defined in Eqn. (4). Under Assumption 5.3, $\Delta_{\text{fair}, \mathcal{L}}^{\text{PS}}(\rho)$ is non-increasing in ρ .*

6 Numerical Results

This section empirically evaluates the proposed methods on synthetic and real-world data (including credit data [4, 23] and MNIST data [24]) under semi-synthesized performative shifts. We run all experiments with multiple random seeds and visualize the standard error with the shaded area. Due to page limits, more experiments are presented in Appendix C.

Performative Gaussian mean estimation. We generate a synthetic dataset of 10000 samples from two groups $s \in \{a, b\}$ with initial group fractions $p_a^{(0)} = 0.3, p_b^{(0)} = 0.7$ and target values $y_a = 0.3 + \epsilon, y_b = 0.7 + \epsilon$, where $\epsilon \sim \mathcal{N}(0, 0.05)$. We consider user retention dynamics where the group fraction $p_s^{(t+1)} = \frac{\mathcal{R}(s, t)}{\sum_{s' \in \{a, b\}} \mathcal{R}(s', t)}$ changes based on group-wise loss. Here

$$\mathcal{R}(s, t) = \left(1 - \sum_{s' \in \{a, b\}} p_{s'}^{\min}\right) \times \frac{1}{2} \left(p_s^t + \frac{\mathcal{L}(\theta^{(t)}; \mathcal{D}_{-s}^{(t)})}{\mathcal{L}(\theta^{(t)}; \mathcal{D}_{-s}^{(t)}) + \mathcal{L}(\theta^{(t)}; \mathcal{D}_s^{(t)})} \right) + p_s^{\min}$$

where $p_s^{\min} = 0.02$ is the minimum group fraction that ensures the sensitivity of the transition mapping T is bounded, and $-s = \{a, b\} \setminus s$. We perform the mean estimation task and train multiple linear regression models using RERM and Fair-RERM, including regularization methods with group-level penalty (Fair-RERM-GLP), sample-level penalty (Fair-RERM-SLP) and sample re-weighting method (Fair-RERM-RW). We perform 30 rounds of empirical risk minimization on 7 different random seeds.

Fig. 2a illustrates the evolution of group-wise loss disparity $\Delta_{\mathcal{L}}^{(t)}$ and Fig. 2b shows the evolution of the minority group fraction (i.e., the group with the lower fraction at the stable point). The blue lines in both figures demonstrate that the PS solution of the regular RERM has the highest unfairness and the most polarized group fractions, while the Fair-PS solution is fairer and the higher ρ results in stronger fairness, implying Fair-RERM is effective in mitigating polarization effects and unfairness. We also note that among all three methods, the sample re-weighting method (Fair-RERM-RW) seems to yield better fairness control than others under this setting.

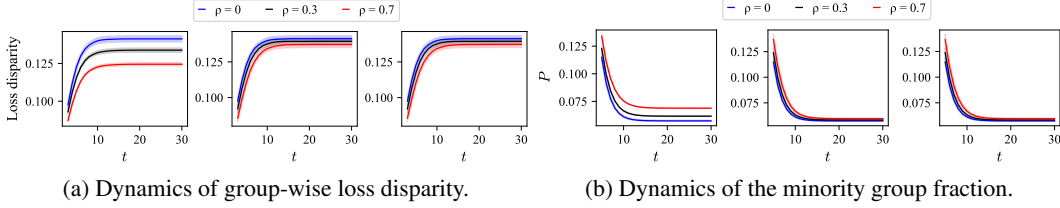


Figure 2: Dynamics of unfairness under **Synthetic** data when $\rho \in \{0, 0.3, 0.7\}$ ($\rho = 0$ is RERM): Fair-RERM-RW (left plot), Fair-RERM-GLP (middle plot), Fair-RERM-SLP (right plot)

Credit data retention dynamics with strategic behaviors. We use the *Give me some credit* data [23] consisting of features $X \in \mathbb{R}^{10}$ to measure individuals' creditworthiness $Y \in \{0, 1\}$ which has been widely used in performative prediction and strategic classification literature [4, 15]. We preprocessed the data similarly to Perdomo et al. [4] and divided individuals into two groups $s \in \{a, b\}$ based on the age attribute. Next, we assume there is a newly established credit rating agency performing RERM and Fair-RERM with logistic classification models to predict individuals' creditworthiness. Similar to the previous experiment, we assume the group-wise loss in round t will affect the group fraction at $t + 1$. Meanwhile, we assume there is a subset of features $X_s \in X$ which individuals can change strategically to X'_s based on the current model parameters θ . Specifically, $X'_s = X_s - \epsilon \cdot \theta_s$, where θ_s is the subset of θ with respect to X_s and $\epsilon = 0.1$. With the dynamics involving both retention and strategic behaviors, we can visualize the dynamics of unfairness under RERM and Fair-RERM in Fig. 3. All results demonstrate the effectiveness of our methods. The regularization method with sample level penalty (Fair-RERM-SLP) seems to be more effective under this setting.

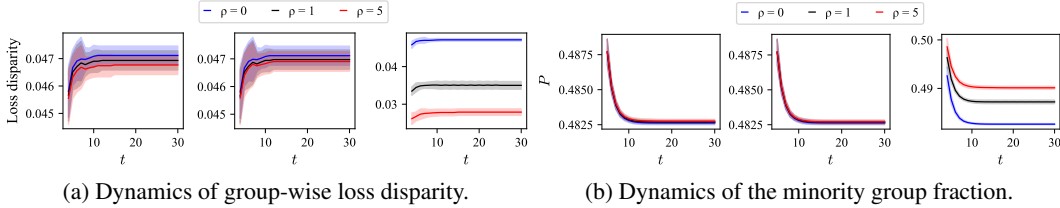


Figure 3: Dynamics of unfairness under **Credit** data when $\rho \in \{0, 1.0, 5.0\}$ ($\rho = 0$ is RERM): Fair-RERM-RW (left plot), Fair-RERM-GLP (middle plot), Fair-RERM-SLP (right plot)

Performative MNIST classification. We next consider MNIST data [24] consisting of handwritten digits images. We randomly select 1000 images as the training set and divide them into 2 groups, where the first group contains all images with digits from 0 to 4 and the second includes digits from 5 to 9. We consider the same group fraction dynamics as before with $p_s^{\min} = 0.1$ for both groups. Using a 2-layer MLP (the loss function violates conditions in Lemma 2.4) for risk minimization, we perform RERM and Fair-RERM for 50 rounds. Fig. 4a and 4b verify that Fair-RERM can still improve fairness at the PS solution. Both plots demonstrate that unfairness is the largest without fairness interventions and Fair-RERM is more effective with larger ρ . Unlike the experiments on synthetic and credit data, this set of experiments does not have a convergence guarantee because conditions for theorems are violated under 2-layer MLP, e.g., the black and red lines ($\rho = 0.3$) of Fair-RERM-RW and Fair-RERM-GLP are unstable. However, the results suggest that our fairness mechanisms may still be useful in practice with deep learning models.

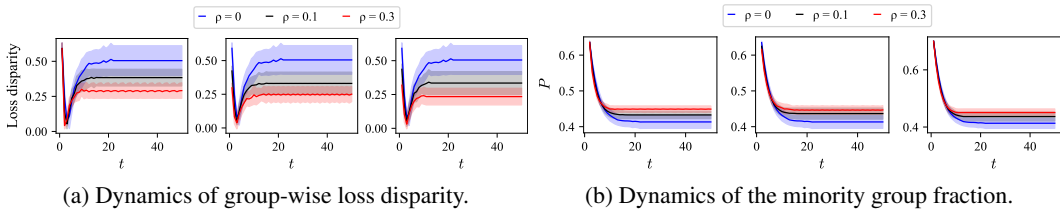


Figure 4: Dynamics of unfairness under **MNIST** data when $\rho \in \{0, 0.1, 0.3\}$ ($\rho = 0$ is RERM): Fair-RERM-RW (left plot), Fair-RERM-GLP (middle plot), Fair-RERM-SLP (right plot)

7 Conclusions & Societal Impacts

Our work reveals the unfairness issues of the PS solutions of PP. We then propose novel fairness-aware algorithms to find Fair-PS solutions with the convergence holds under mild assumptions, which will facilitate trustworthy machine learning since PP has broad applications on human-related decisions ranging from college admission and loan approval to hiring practice. Meaningful future directions include relaxing the conditions for the convergence of fairness mechanisms or expanding the mechanisms to deep learning settings.

References

- [1] Moritz Hardt, Nimrod Megiddo, Christos Papadimitriou, and Mary Wootters. Strategic Classification, November 2015. URL <http://arxiv.org/abs/1506.06980>. Number: arXiv:1506.06980 arXiv:1506.06980 [cs].
- [2] Xueru Zhang, Mohammad Mahdi Khalili, Cem Tekin, and Mingyan Liu. *Group Retention When Using Machine Learning in Sequential Decision Making: The Interplay between User Dynamics and Fairness*. Curran Associates Inc., Red Hook, NY, USA, 2019.
- [3] Jianfeng Chi, Jian Shen, Xinyi Dai, Weinan Zhang, Yuan Tian, and Han Zhao. Towards return parity in markov decision processes. In *International Conference on Artificial Intelligence and Statistics*, pages 1161–1178. PMLR, 2022.
- [4] Juan C. Perdomo, Tijana Zrnic, Celestine Mendler-Dünner, and Moritz Hardt. Performative Prediction. *arXiv:2002.06673 [cs, stat]*, February 2021. URL <http://arxiv.org/abs/2002.06673>. arXiv: 2002.06673.
- [5] Gavin Brown, Shlomi Hod, and Iden Kalemaj. Performative prediction in a stateful world. In Gustau Camps-Valls, Francisco J. R. Ruiz, and Isabel Valera, editors, *Proceedings of The 25th International Conference on Artificial Intelligence and Statistics*, volume 151 of *Proceedings of Machine Learning Research*, pages 6045–6061. PMLR, 28–30 Mar 2022. URL <https://proceedings.mlr.press/v151/brown22a.html>.
- [6] Natalia Martinez, Martin Bertran, and Guillermo Sapiro. Minimax pareto fairness: A multi objective perspective. In *International conference on machine learning*, pages 6755–6764. PMLR, 2020.
- [7] Emily Diana, Wesley Gill, Michael Kearns, Krishnaram Kenthapadi, and Aaron Roth. Minimax group fairness: Algorithms and experiments. In *Proceedings of the 2021 AAAI/ACM Conference on AI, Ethics, and Society*, pages 66–76, 2021.
- [8] Reilly Raab, Ross Boczar, Maryam Fazel, and Yang Liu. Fair participation via sequential policies. *Proceedings of the AAAI Conference on Artificial Intelligence*, pages 14758–14766, 2024.
- [9] Falaah Arif Khan, Denys Herasymuk, and Julia Stoyanovich. On fairness and stability: Is estimator variance a friend or a foe? *arXiv preprint arXiv:2302.04525*, 2023.
- [10] Fengda Zhang, Kun Kuang, Yuxuan Liu, Long Chen, Chao Wu, Fei Wu, Jiaxun Lu, Yunfeng Shao, and Jun Xiao. Unified group fairness on federated learning. *arXiv preprint arXiv:2111.04986*, 2021.
- [11] Sangwon Jung, Taeon Park, Sanghyuk Chun, and Taesup Moon. Re-weighting based group fairness regularization via classwise robust optimization, 2023.
- [12] John Duchi and Hongseok Namkoong. Learning models with uniform performance via distributionally robust optimization. *arXiv preprint arXiv:1810.08750*, 2018.
- [13] John Duchi, Tatsunori Hashimoto, and Hongseok Namkoong. Distributionally robust losses for latent covariate mixtures. *Operations Research*, 71(2):649–664, 2023.
- [14] Sebastian Zetzka and Konstantin Genin. Performativity and prospective fairness. *arXiv preprint arXiv:2310.08349*, 2023.

- [15] Yaowei Hu and Lu Zhang. Achieving long-term fairness in sequential decision making. In *Proceedings of the AAAI Conference on Artificial Intelligence*, volume 36, pages 9549–9557, 2022.
- [16] Kun Jin, Xueru Zhang, Mohammad Mahdi Khalili, Parinaz Naghizadeh, and Mingyan Liu. Incentive mechanisms for strategic classification and regression problems. In David M. Pennock, Ilya Segal, and Sven Seuken, editors, *EC '22: The 23rd ACM Conference on Economics and Computation, Boulder, CO, USA, July 11 - 15, 2022*, pages 760–790. ACM, 2022. doi: 10.1145/3490486.3538300. URL <https://doi.org/10.1145/3490486.3538300>.
- [17] Xueru Zhang, Mohammad Mahdi Khalili, Kun Jin, Parinaz Naghizadeh, and Mingyan Liu. Fairness interventions as (Dis)Incentives for strategic manipulation. In Kamalika Chaudhuri, Stefanie Jegelka, Le Song, Csaba Szepesvari, Gang Niu, and Sivan Sabato, editors, *Proceedings of the 39th International Conference on Machine Learning*, volume 162 of *Proceedings of Machine Learning Research*, pages 26239–26264. PMLR, 17–23 Jul 2022. URL <https://proceedings.mlr.press/v162/zhang221.html>.
- [18] Tatsunori Hashimoto, Megha Srivastava, Hongseok Namkoong, and Percy Liang. Fairness without demographics in repeated loss minimization. In Jennifer Dy and Andreas Krause, editors, *Proceedings of the 35th International Conference on Machine Learning*, volume 80 of *Proceedings of Machine Learning Research*, pages 1929–1938. PMLR, 10–15 Jul 2018. URL <https://proceedings.mlr.press/v80/hashimoto18a.html>.
- [19] Tatsunori Hashimoto, Megha Srivastava, Hongseok Namkoong, and Percy Liang. Fairness without demographics in repeated loss minimization. In *International Conference on Machine Learning*, pages 1929–1938. PMLR, 2018.
- [20] Jon Kleinberg and Manish Raghavan. How do classifiers induce agents to invest effort strategically?, 2019.
- [21] Liam Peet-Pare, Nidhi Hegde, and Alona Fyshe. Long term fairness for minority groups via performative distributionally robust optimization, 2022.
- [22] Garnet Liam Peet-Pare, Nidhi Hegde, and Alona Fyshe. Long term fairness via performative distributionally robust optimization, 2023. URL <https://openreview.net/forum?id=YvrAyFZq0ID>.
- [23] Kaggle. Give me some credit. <https://www.kaggle.com/c/GiveMeSomeCredit/data>, 2012.
- [24] Li Deng. The mnist database of handwritten digit images for machine learning research. *IEEE Signal Processing Magazine*, 29(6):141–142, 2012.
- [25] Reilly Raab and Yang Liu. Unintended selection: Persistent qualification rate disparities and interventions. *Advances in Neural Information Processing Systems*, 34, 2021.
- [26] Tian Xie, Xuwei Tan, and Xueru Zhang. Algorithmic decision-making under agents with persistent improvement, 2024.
- [27] Tian Xie, Zhiqun Zuo, Mohammad Mahdi Khalili, and Xueru Zhang. Learning under imitative strategic behavior with unforeseeable outcomes, 2024.
- [28] Danielle Ensign, Sorelle A Friedler, Scott Neville, Carlos Scheidegger, and Suresh Venkatasubramanian. Runaway feedback loops in predictive policing. In *Conference on fairness, accountability and transparency*, pages 160–171. PMLR, 2018.
- [29] Celestine Mender-Dünner, Juan Perdomo, Tijana Zrnic, and Moritz Hardt. Stochastic optimization for performative prediction. In *Advances in neural information processing systems*, pages 4929–4939. Curran Associates, Inc., 2020.
- [30] Mehrnaz Mofakhami, Ioannis Mitliagkas, and Gauthier Gidel. Performative prediction with neural networks. In *International Conference on Artificial Intelligence and Statistics*, pages 11079–11093. PMLR, 2023.

- [31] Yulai Zhao. Optimizing the performative risk under weak convexity assumptions. *arXiv preprint arXiv:2209.00771*, 2022.
- [32] John Miller, Juan C. Perdomo, and Tijana Zrnic. Outside the Echo Chamber: Optimizing the Performative Risk. *arXiv:2102.08570 [cs, stat]*, June 2021. URL <http://arxiv.org/abs/2102.08570>. arXiv: 2102.08570.
- [33] Zachary Izzo, Lexing Ying, and James Zou. How to learn when data reacts to your model: Performative gradient descent. *CoRR*, 2021. arXiv: 2102.07698.
- [34] Moritz Hardt and Celestine Mendler-Dünner. Performative prediction: Past and future. *arXiv preprint arXiv:2310.16608*, 2023.
- [35] Toshihiro Kamishima, Shotaro Akaho, and Jun Sakuma. Fairness-aware learning through regularization approach. In *2011 IEEE 11th International Conference on Data Mining Workshops*, pages 643–650, 2011. doi: 10.1109/ICDMW.2011.83.
- [36] Muhammad Bilal Zafar, Isabel Valera, Manuel Gomez Rodriguez, and Krishna P Gummadi. Fairness beyond disparate treatment & disparate impact: Learning classification without disparate mistreatment. In *Proceedings of the 26th international conference on world wide web*, pages 1171–1180, 2017.
- [37] Ozgur Guldogan, Yuchen Zeng, Jy-yong Sohn, Ramtin Pedarsani, and Kangwook Lee. Equal improvability: A new fairness notion considering the long-term impact. *arXiv preprint arXiv:2210.06732*, 2022.
- [38] Smitha Milli, John Miller, Anca D. Dragan, and Moritz Hardt. The social cost of strategic classification, 2018.
- [39] Lily Hu, Nicole Immorlica, and Jennifer Wortman Vaughan. The disparate effects of strategic manipulation. In *ACM Conference on Fairness, Accountability, and Transparency*, Atlanta, Georgia, 2019.
- [40] Xueru Zhang, Ruibo Tu, Yang Liu, Mingyan Liu, Hedvig Kjellström, Kun Zhang, and Cheng Zhang. How do fair decisions fare in long-term qualification? In *Proceedings of the 34th International Conference on Neural Information Processing Systems, NIPS’20*, Red Hook, NY, USA, 2020. Curran Associates Inc. ISBN 9781713829546.
- [41] Sébastien Bubeck. Convex optimization: Algorithms and complexity. *Found. Trends Mach. Learn.*, 8(3–4):231–357, nov 2015. ISSN 1935-8237. doi: 10.1561/22000000050. URL <https://doi.org/10.1561/22000000050>.
- [42] Nicolas Fournier and Arnaud Guillin. On the rate of convergence in Wasserstein distance of the empirical measure. *Probability Theory and Related Fields*, 162(3-4):707, August 2015. URL <https://hal.science/hal-00915365>.

A Related Works

Performative Prediction. Proposed by Perdomo et al. [4], Performative prediction focuses on machine learning problems where the model deployments influence the data distribution, and the common application scenarios include strategic classification [1, 25, 26, 27] and predictive policing [28]. Perdomo et al. [4] formulated the problem and proposed *repeated risk minimization* (RRM) to ensure the convergence of model parameters to a stable point under a set of sufficient and necessary conditions. Mendler-Dünner et al. [29] presented convergence results on stochastic performative optimization. Subsequent work either strived to relax the convergence condition [30, 31] or develop methods to ensure the convergence to performative optimal points under special cases [32, 33]. Brown et al. [5] extended performative prediction to stateful settings where the current data distribution is determined by both the previous states and the deployed model. For more related works on PP, we refer to this survey [34].

Long-term fairness. There is a large line of work on long-term fairness in machine learning, where we mainly refer to distributionally robust optimization (DRO) [12, 13] and soft fair regularizers [35, 36, 37]. DRO refers to the optimization problem where the loss is minimized on the worst-case distribution around current data distribution [12, 13], while soft fair regularizers are often used in traditional fair optimization frameworks to penalize unfairness. Only a few pieces of literature touched on fairness problems under performative prediction settings. [17, 38, 39, 40] focused on long-term fairness settings under strategic classification similar to Example 3.2. Zezulka and Genin [14] pointed out fairness issues in performative prediction and formulated it within causal graphs. Hu and Zhang [15] also used causality-based models to formulate and ensure short-term and long-term fairness in performative prediction, incurring strong assumptions and expensive computational costs. Raab et al. [8] studied a special case where only the agents’ retention rates are performative. Peet-Pare et al. [21] proposed to use distributionally robust optimization (DRO) to promote fairness in performative prediction, but they proposed assumptions that are hard to verify and can not be derived from other commonly accepted assumptions in PP.

B Further Elaboration on the Concepts

Here we include the notation table and a Venn diagram to help the readers better understand the technical details of our paper.

B.1 Notation Table

B.2 Venn Diagram of Concepts in PP

We present a Venn diagram of different PP cases in Figure 5. Within the broad concept of PP, we specifically characterize 3 practical concepts in real-world problems, namely the (1) state-dependent performative shifts, (2) performative retention dynamics, and (3) performative distribution shifts. These concepts represent different dimensions to partition the PP problems.

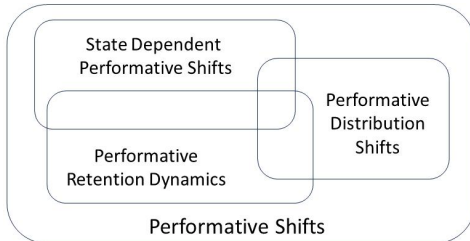


Figure 5: A Venn diagram of the PP cases.

Performative Retention Dynamics (PRD). Previous works that study long-term fairness [2, 40] mostly assume there to be model-dependent retention rate/population fraction p_s changes, which can all be formulated as PRD problems. Recommendation systems are typical application scenarios

Notation	Meanings
θ	Model parameters
h_θ	The decision model parameterized by θ
Θ	The parameter space
Z	Data sample
X	Feature in the data sample
Y	Label in the data sample
\mathcal{D}	Sample distribution
$\Delta(\mathcal{Z})$	Support of sample distribution
\mathbf{T}	Transition mapping
\mathbf{T}^k	k -Delayed transition mapping
\mathbf{T}^{DL}	Delayed transition mapping where $k = \lceil r \rceil + 1$
ℓ	Loss function
s	Sensitive attribute, where group s means the set of samples with attribute s
\mathcal{S}	The set of sensitive attributes
\mathcal{L}_s	The expected loss of group s
$\mathcal{D}_s^{(t)}$	Sample distribution of group s at time t
$p_s^{(t)}$	Population fraction of group s at time t
\mathcal{W}_1	The 1-Wasserstein distance
$\Delta_{DP}, \Delta_{EO}, \Delta_{\mathcal{L}}$	Demographic Parity, Equal Opportunity, Loss Disparity penalty
$\mathcal{L}_{\text{fair}}$	Fairness-aware objective
\mathcal{P}	The penalty term in fairness aware objective
\mathcal{B}	Distribution ball, used to limit the choices of re-weighting
$\mathbf{l}^{(t)}$	Loss-guided re-weighting vector for time step t
$q_s^{(t)}$	Group weight of group s at time t in the fair reweighting mechanism
ρ	Strength of fair mechanism
γ	Strong convexity coefficient of the loss
β	Joint smoothness coefficient of the loss
ϵ	Joint sensitivity coefficient of the transition mapping
$\tilde{\beta}$	Joint smoothness coefficient of the fairness-aware objective
$\bar{\ell}$	Maximum loss value given Θ and $\Delta(\mathcal{Z})$

Table 1: Summary of notation.

of SDPP and PRD since the population fraction in the next iteration depends on both the current population and the current model. The better recommendation model captures a certain user group’s interest, the more likely this user group will have high retention rate.

Example B.1. (User retention) Suppose two demographic groups a, b each follow a static distribution \mathcal{D}_a and \mathcal{D}_b , but their fraction in the population changes over time, and thus the overall data

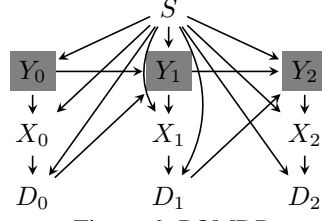


Figure 6: POMDP

distribution is dynamic. Specifically, let p_s^{min} be control variables to limit the minimum fraction of group s , and their retention rate is determined by a retention function $\pi_s(\boldsymbol{\theta}^{(t)})$. Then we have

$$p_s^{(t)} := \frac{p_s^{(t-1)}\pi_s(\boldsymbol{\theta}^{(t)}) + p_s^{min}}{\sum_{s'}(p_{s'}^{(t-1)}\pi_{s'}(\boldsymbol{\theta}^{(t)}) + p_{s'}^{min})}, \quad \mathcal{D}^{(t)} = \sum_s p_s^{(t)}\mathcal{D}_s, \quad (10)$$

which can be modeled by PP in the SDPP setting.

Performative Distribution Shifts (PDS). In this paper, PDS specifically means in each group, the data distribution \mathcal{D}_s shifts with the decision models, e.g., in strategic classification, users strategically manipulate their features for better decision outcomes. In recommendation systems, where creators strategically manipulate their features for better decision outcomes from the model [1], and users' interests can be shifted by the recommended items.

We present a practical example of PP in addition to the one in the main article.

Example B.2. (Partially observable Markov decision process (POMDP) as PDS [40]) The population fractions of the two groups p_s are static, i.e., $\mathcal{D}^{(t)} = \sum_s p_s \mathcal{D}_s^{(t)}$, but the feature distribution changes with the deployed decision model, and such changes follow a POMDP as shown in Figure 6.

Specifically, within each group, there are two sub-populations, qualified and disqualified, e.g., the qualified sub-population in group a satisfies $y = 1, s = a$. Each sub-population has a static distribution, $\mathcal{D}_{s,y}$, but each group's distribution is dynamic and determined by

$$\mathcal{D}_s^{(t)} = \sum_y \alpha_{s,y}^{(t)} \mathcal{D}_{s,y}, \quad \alpha_{s,y}^{(t)} := \mathbb{P}(Y^{(t)} = 1 | S = s), \quad (11)$$

where $Y^{(t)}$ is the random variable of the agent's true label at time step t . The POMDP assumes the decision model and the sensitive attribute jointly determine the distribution of the true label distribution at the next time step, and we have

$$\alpha_{s,1}^{(t)} = \sum_{y=0}^1 \alpha_{s,y}^{(t-1)} \underbrace{\mathbb{P}(Y^{(t)} = 1 | Y^{(t-1)} = y, \boldsymbol{\theta} = \boldsymbol{\theta}^{(t)}, S = s)}_{\text{from POMDP}}, \quad (12)$$

and we can similarly write out the dynamics of all the $\alpha_{s,y}^{(t)}$ terms and thus the transition mapping T as a PDS problem.

B.3 Fair-RERM

Here we provide the algorithm for the Fair-RERM class and the results of its sample complexity.

Algorithm 2 Fair-RERM

Input: $t = 0, \mathcal{D}^{(0)}, \rho, \boldsymbol{\theta}^{(0)}, \delta_\theta$, choose fair mechanism

repeat

 Sample $\mathcal{Z}^{(t)}$ from $\mathcal{D}^{(t)}$

$\boldsymbol{\theta}^{(t+1)} \leftarrow \arg \min_{\boldsymbol{\theta}} \mathcal{L}_{\text{fair}}(\boldsymbol{\theta}; \mathcal{Z}^{(t)}, \rho)$

 Get the samples from $\mathcal{D}^{(t+1)}$ changing according to different schema

$t \leftarrow t + 1$

until $\|\boldsymbol{\theta}^{(t)} - \boldsymbol{\theta}^{(t-1)}\|_2 \leq \delta_\theta$

Theorem B.3 (Convergence of fair-RERM). *Suppose $\exists \alpha > 1, \mu > 0$ such that $\int_{\mathbb{R}^m} e^{\mu|x|^\alpha} Z dx$ is finite $\forall Z \in \Delta(\mathcal{Z})$. For a given convergence radius $\delta \in (0, 1)$, take $n_t = \mathcal{O}\left(\frac{\log(t/p)}{(\epsilon(1+\tilde{\beta}/\gamma)\delta)^m}\right)$ samples at t . If $2\epsilon(1 + \tilde{\beta}/\gamma) < 1$, then with probability $1 - p$, the iterates of fair-RERM are within a radius δ of the Fair-PS solution for $t \geq (1 - 2\epsilon(1 + \tilde{\beta}/\gamma))\mathcal{O}(\log(1/\delta))$.*

B.4 General guidance of designing fairness objectives under the SDPP setting

The key to designing a fairness objective while ensuring the convergence of the iterative algorithm is to ensure the convexity of the fairness penalty. Example 4.2 shows that group loss variance cannot preserve the convexity of $\mathcal{L}_{\text{fair}}$, so it fails to be a plausible objective. This implies that each penalty term in terms of $P = g(\mathcal{L})$ where the convexity of P is ensured can be a fairness objective. However, it can still be highly non-trivial to design a fair objective in this form due to the following reasons: (i) it is hard to design an objective as interpretable as the ones we mentioned in Section 4. The squared loss as a penalty term is well-motivated and directly penalizes the groups/samples with the higher losses; (ii) It becomes more difficult to obtain the concrete parameters for the convergence guarantee. For example, $\bar{\ell}$ in Section 5 becomes the upper bound of $\frac{\partial g}{\partial \ell}$ and this may be hard to obtain and interpret. Overall, we see the formulations in Section 4 as more appropriate choices.

B.5 Only Measure Fairness at PS Solution

We provide an example to illustrate that fairness is not guaranteed even if we ensure instantaneous fairness without stability being achieved.

Example B.4. (*Fairness violation due to performative shifts*) *Consider a binary strategic classification problem with two groups a, b and is a threshold model $h_\theta(X) = \mathbb{1}\{X \geq \theta\}$. p_a, p_b are fixed and both groups satisfy $\mathbb{P}(Y^{(t)} = 1) = \min\{0, \max\{X^{(t)}, 1\}\}$, and the transitions satisfy $X^{(t)} = X^{(0)} + (0.1 + 0.1 \cdot \mathbf{1}\{s = a\})\theta^{(t)}$ but do not result in any changes in labels. If at $t = 0$, both groups have features $X^{(0)}$ subject to uniform distribution on $[0, 1]$, then any $\theta = 0.5$ satisfies accuracy parity. However, at $t = 1$, group a has a shifted distribution, resulting in $\theta = 0.5$ to be unfair.*

C Additional Experiments

All experiments are run on the CPU of a Macbook Pro with Apple M1 Pro chip and 16GB memory. We use Python 3.9 for all tasks. For datasets, Yann LeCun and Corinna Cortes hold the copyright of MNIST, which is a derivative work from original NIST datasets. MNIST dataset is made available under the terms of the Creative Commons Attribution-Share Alike 3.0 license; the credit dataset has been published by Kaggle [23]; In Appendix C.1, we visualize the convergence of performative loss for all the above experiments. In Appendix C.3, we perform experiments on a performative Gaussian data classification task. In Appendix C.2, we conduct experiments on 3 groups. In Appendix C.4, we visualize the unconvergence of the fairness penalty using group loss variance as a complementary to Example 4.2; Finally, we examine the **k-delayed** schema on all our fairness mechanisms on Credit data in Appendix C.5 and obtain the similar results.

C.1 Model Convergence in Main Experiments

In this section, we provide visualizations of the convergence of performative loss for all experiments of the main paper in Fig. 12. Importantly, Fig. 12d demonstrates the unconvergence of Fair-RERM-RW and Fair-RERM-GLP when $\rho = 0.3$.

C.2 Gaussian Mean Estimation with Multiple Groups

In this section, we present the experimental results on the Gaussian mean estimation task with 3 groups $s \in \{a, b, c\}$ where $p_a^{(0)} = 0.15, p_b^{(0)} = 0.25, p_c^{(0)} = 0.6$ with different target values. We let $y_a = 0.3 + \epsilon, y_b = 0.5 + \epsilon, y_c = 0.7 + \epsilon$ where $\epsilon \sim \mathcal{N}(0, 0.05)$. At the beginning, the Group fraction $p_a^{(0)} = 0.3, p_b^{(0)} = 0.7$, and the minimum group fraction for each group is $p^{\text{min}} = \{0.1, 0.1\}$. At

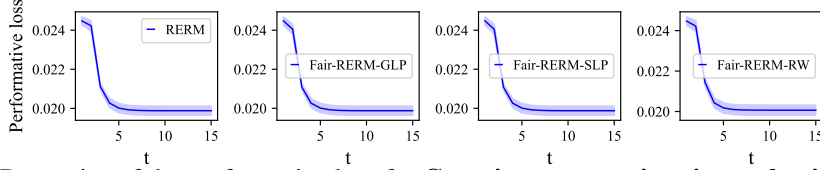


Figure 7: Dynamics of the performative loss for **Gaussian mean estimation task with multiple groups** when $\rho = 0.3$: Fair-RERM-RW (left plot), Fair-RERM-GLP (middle plot), Fair-RERM-SLP (right plot).

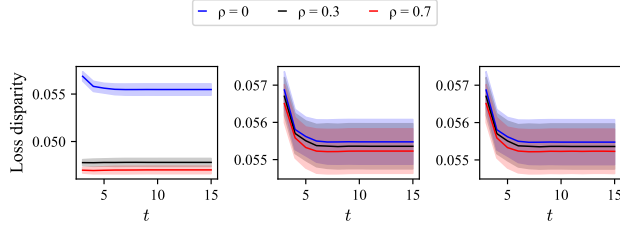


Figure 8: Dynamics of the performative loss disparity under different ρ : Fair-RERM-RW (left plot), Fair-RERM-GLP (middle plot), Fair-RERM-SLP (right plot).

each time t , denote $\mathcal{R}(s, t) = \left(1 - \sum_{s' \in \{a, b\}} p_{s'}^{min}\right) \times \frac{1}{2} \left(p_s^t + \frac{\mathcal{L}(\theta^{(t)}; \mathcal{D}_{i_s}^{(t)})}{\sum_{s'} \mathcal{L}(\theta^{(t)}; \mathcal{D}_{s'}^{(t)})} \right) + p_s^{min}$. $-s$ is the group other than s , while i_s is found by first ranking all group-wise losses in ascending order and then selecting the $(n + 1 - i) - th$ largest loss if group s has the $i - th$ largest loss. This retention dynamic is a direct generalization of the two-group case. Next, we show the retention of group $p_s^{(t+1)}$ at time $t + 1$ is shown as Eqn. (13), resulting in the new data distribution $D^{(t+1)}$.

$$p_s^{(t+1)} := \frac{\mathcal{R}(s, t)}{\sum_{s' \in \{a, b\}} \mathcal{R}(s', t)} \quad (13)$$

We perform the mean estimation task for the whole data distribution with both RERM and Fair-RERM using the linear regression model. For Fair-RERM, we use RERM, Fair-RERM-RW and Fair-RERM to perform 30 rounds of risk minimization where the loss is mean squared error (MSE), and name them as Fair-RERM-GLP (group-level penalty), Fair-RERM-SLP (sample-level penalty) and Fair-RERM-RW (reweighting). We first verify the convergence of performative loss of the above methods in Fig. 7 where all Fair-RERM methods have $\rho = 0.1$. The results demonstrate all methods successfully converge to the PS point.

Next, we verify the effectiveness of Fair-RERM by visualizing the dynamics of performative loss disparity between the groups while varying ρ in Fig. 8, where the higher ρ still results in lower loss disparity at the stable point, revealing that Fair-RERM-RW and Fair-RERM are effective.

C.3 Performative Gaussian data classification.

We use a synthetic dataset consisting of 1000 samples from 2 demographic groups $s \in \{a, b\}$ with features $X = \{X_1, X_2\}$ and labels $Y \in \{0, 1\}$. For group a , $Y = \mathbb{1}\{x_1 - 0.5x_2 \geq 0.5\}$. For group b , $Y = \mathbb{1}\{0.5x_1 + 0.5x_2 \geq 0.5\}$. The initial group fraction and the retention mapping are the same as in the previous experiment. Using a logistic classification model for risk minimization, we first verify the convergence of performative loss in Fig. 9 and the effectiveness of Fair-RERM-RW and Fair-RERM in Fig. 13a and Fig. 13b. All plots demonstrate the same trends as the previous experiment.

C.4 Gaussian Mean Estimation Using Group Loss Variance

In Example 4.2, we already prove that group loss variance as a fair penalty term violates the strong convexity assumption. In this section, we show its unconvergence while performing the Gaussian

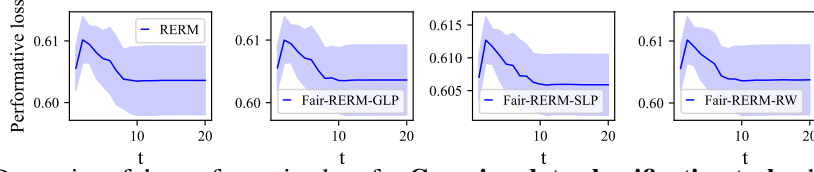


Figure 9: Dynamics of the performative loss for **Gaussian data classification task** when $\rho = 0.3$: Fair-RERM-RW (left plot), Fair-RERM-GLP (middle plot), Fair-RERM-SLP (right plot).

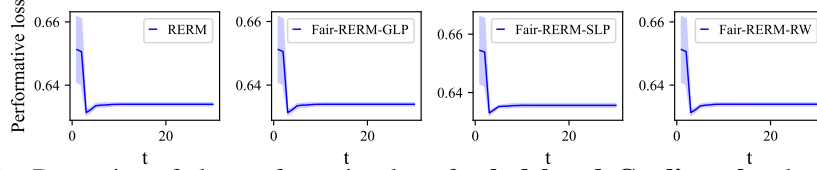


Figure 10: Dynamics of the performative loss for **k-delayed Credit task** when $\rho = 0.3$: Fair-RERM-RW (left plot), Fair-RERM-GLP (middle plot), Fair-RERM-SLP (right plot).

mean estimation task under the same setting mentioned in Section 6 when $\rho = 0.5$. The dynamics of $\|\theta_t - \theta_{t-1}\|$ as well as performative loss are shown as follows. Fig. 11 shows the unconvergence, which is contradicted to Fig. 12a where we show the convergence of Fair-RERM.

C.5 K-delayed RERM on Credit Data

We examine the effectiveness of k-delayed RERM schema on Credit Data [23] which is the same dataset used by Brown et al. [5]. Specifically, we use $k = 3$ and $\epsilon = 1$ to form equal-sized agent groups uniformly in the whole population to let each subgroup best respond with different speed (Example 1 in Brown et al. [5]). We also let the retention dynamic be k-delayed, adding additional challenges compared to the previous work. We examine $\rho \in \{0.3, 0.7\}$ while all other settings are the same as the Credit Data experiment in Section 6.

Then we first verify the convergence of performative loss in Fig. 9 and the effectiveness of k-delayed Fair-RERM-RW and Fair-RERM in Fig. 13a and Fig. 13b. All plots demonstrate the same trends as the previous experiment with RRM schema.

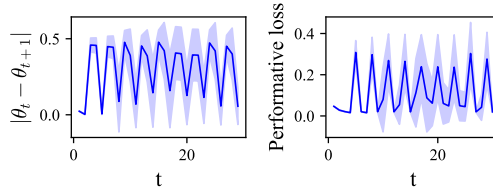
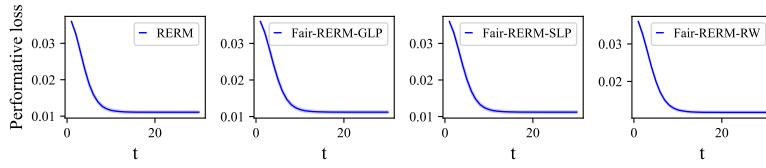
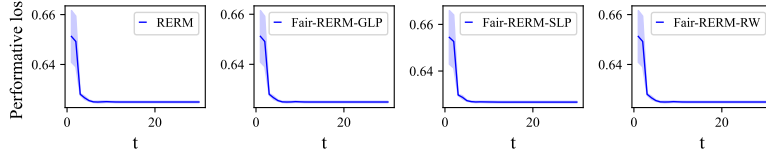


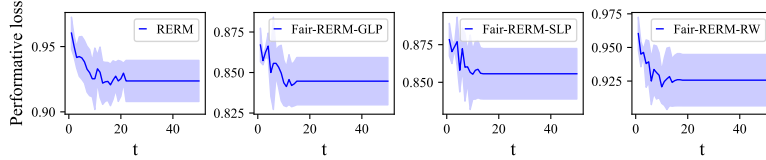
Figure 11: Gaussian mean estimation using group loss variance



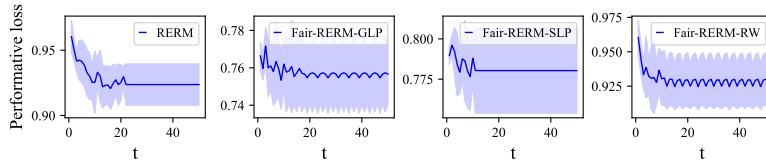
(a) Dynamics of the performative loss for **Gaussian mean estimation task** when $\rho = 0.1$: Fair-RERM-RW (left plot), Fair-RERM-GLP (middle plot), Fair-RERM-SLP (right plot).



(b) Dynamics of the performative loss for **Credit data task** when $\rho = 0.1$: Fair-RERM-RW (left plot), Fair-RERM-GLP (middle plot), Fair-RERM-SLP (right plot).

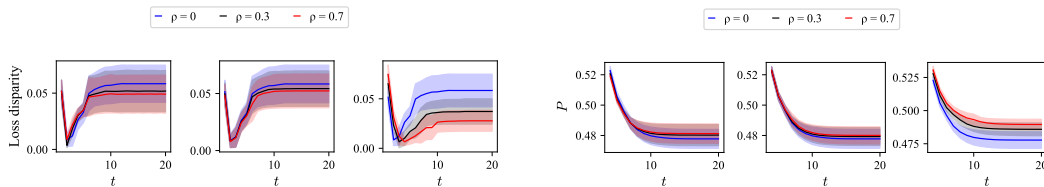


(c) Dynamics of the performative loss for **MNIST classification task** when $\rho = 0.1$: Fair-RERM-RW (left plot), Fair-RERM-GLP (middle plot), Fair-RERM-SLP (right plot).



(d) Dynamics of the performative loss for **MNIST classification task** when $\rho = 0.3$: Fair-RERM-RW (left plot), Fair-RERM-GLP (middle plot), Fair-RERM-SLP (right plot).

Figure 12: Performative loss dynamics under different ρ



(a) Dynamics of the loss disparity under different ρ : Fair-RERM-RW (left plot), Fair-RERM-GLP (middle plot), Fair-RERM-SLP (right plot).

(b) Dynamics of the minority group fraction under different ρ : Fair-RERM-RW (left plot), Fair-RERM-GLP (middle plot), Fair-RERM-SLP (right plot).

Figure 13: Fairness dynamics of Performative Gaussian Classification where $\rho \in \{0, 0.3, 0.7\}$ ($\rho = 0$ is equivalent to RERM)

D Proofs for the Theoretical Results

D.1 Proof of Proposition 5.1

We will first present lemmas for this proposition.

Lemma D.1. (First order optimality condition of convex functions [41]).

If f is convex and Ω is a closed convex set on which f is differentiable, then

$$x^* \in \arg \min_{x \in \Omega} f(x), \quad (14)$$

if and only if $(y - x^*)^\top \nabla g(x^*) \geq 0$ for all $y \in \Omega$.

Lemma D.2. ($\mathcal{L}_{\text{fair}}$ under fair penalty mechanisms is γ -strongly convex)

Under the conditions in Lemma 2.4, the loss aware objective $\mathcal{L}_{\text{fair}}$ in Eqn (7) and (8) are γ -strongly convex.

Proof. We will show this for the sample level fair penalty Eqn (8) first.

From conditions in Lemma 2.4, we know that ℓ is γ -strongly convex, and by definition $\ell \geq 0$, we will show that $\ell^2(\boldsymbol{\theta}; Z)$ is also convex in $\boldsymbol{\theta}$. For simplicity of notation, we will derive for an arbitrary fixed Z and omit Z in the following derivation and use $\ell(\boldsymbol{\theta})$.

From the definition of convexity, we have $\forall \alpha \in (0, 1), \forall \boldsymbol{\theta}_1, \boldsymbol{\theta}_2 \in \Theta$,

$$\ell((1 - \alpha)\boldsymbol{\theta}_1 + \alpha\boldsymbol{\theta}_2) \leq (1 - \alpha)\ell(\boldsymbol{\theta}_1) + \alpha\ell(\boldsymbol{\theta}_2). \quad (15)$$

Squaring both sides in the above gives us

$$\begin{aligned} \ell^2((1 - \alpha)\boldsymbol{\theta}_1 + \alpha\boldsymbol{\theta}_2) &\leq (1 - \alpha)^2\ell^2(\boldsymbol{\theta}_1) + \alpha^2\ell^2(\boldsymbol{\theta}_2) + 2\alpha(1 - \alpha)\ell(\boldsymbol{\theta}_1)\ell(\boldsymbol{\theta}_2) \\ &= (1 - \alpha)^2\ell^2(\boldsymbol{\theta}_1) + \alpha^2\ell^2(\boldsymbol{\theta}_2) + 2\alpha(1 - \alpha)\ell(\boldsymbol{\theta}_1)\ell(\boldsymbol{\theta}_2) \\ &\quad - (1 - \alpha)\ell^2(\boldsymbol{\theta}_1) - \alpha\ell^2(\boldsymbol{\theta}_2) + (1 - \alpha)\ell^2(\boldsymbol{\theta}_1) + \alpha\ell^2(\boldsymbol{\theta}_2) \\ &= -\alpha(1 - \alpha)[\ell(\boldsymbol{\theta}_1) - \ell(\boldsymbol{\theta}_2)]^2 + (1 - \alpha)\ell^2(\boldsymbol{\theta}_1) + \alpha\ell^2(\boldsymbol{\theta}_2) \\ &\leq (1 - \alpha)\ell^2(\boldsymbol{\theta}_1) + \alpha\ell^2(\boldsymbol{\theta}_2), \end{aligned} \quad (16)$$

which shows the convexity of ℓ^2 .

Therefore, $\ell(\boldsymbol{\theta}) + \rho\ell^2(\boldsymbol{\theta})$ is a sum of a γ -strongly convex function and a convex function and thus is γ -strongly convex. Then since $\mathcal{L}_{\text{fair}}$ is an affine combination of γ -strongly convex functions, it is also γ -strongly convex.

For Eqn (7), since \mathcal{L}_s is γ -strongly convex for $\forall s$, we can similarly show $\mathcal{L}_{\text{fair}}$ is γ -strongly convex. \square

Lemma D.3. ($\mathcal{L}_{\text{fair}}$ under fair penalty mechanisms is $\tilde{\beta}$ -jointly smooth)

Under conditions in Lemma 2.4, the loss aware objective $\mathcal{L}_{\text{fair}}$ in Eqn (7) and (8) are $\tilde{\beta}$ -jointly smooth, where $\tilde{\beta} = (2\rho\bar{\ell} + 1)\beta$.

Proof. Denote $g := \ell^2$, then we have $\nabla_{\boldsymbol{\theta}} g = 2\ell \cdot \nabla_{\boldsymbol{\theta}} \ell$, and thus we have

$$\begin{aligned} \|\nabla_{\boldsymbol{\theta}} g(\boldsymbol{\theta}; Z) - \nabla_{\boldsymbol{\theta}} g(\boldsymbol{\theta}'; Z)\|_2 &\leq 2\beta \max\{\ell(\boldsymbol{\theta}; Z), \ell(\boldsymbol{\theta}'; Z)\} \|\boldsymbol{\theta} - \boldsymbol{\theta}'\|_2, \\ \|\nabla_{\boldsymbol{\theta}} g(\boldsymbol{\theta}; Z) - \nabla_{\boldsymbol{\theta}} g(\boldsymbol{\theta}; Z')\|_2 &\leq 2\beta \max\{\ell(\boldsymbol{\theta}; Z), \ell(\boldsymbol{\theta}; Z')\} \|Z - Z'\|_2, \end{aligned} \quad (17)$$

which implies $(2\rho\bar{\ell} + 1)\beta$ -joint smoothness of $\mathcal{L}_{\text{fair}}$ in Eqn (7) and (8). \square

Lemma D.4. For fair re-weighting mechanisms,

$$\boldsymbol{\theta}^{(t+1)} = \arg \min_{\boldsymbol{\theta}} \mathcal{L}_{\text{fair}} = \arg \min_{\boldsymbol{\theta}} \sum_s p_s^{(t)} (1 + \rho\mathcal{L}_s(\boldsymbol{\theta}^{(t)}; \mathcal{D}_s^{(t-1)})\mathcal{L}_s(\boldsymbol{\theta}); \mathcal{D}_s^{(t)}), \quad (18)$$

where $\sum_s p_s^{(t)} (1 + \rho\mathcal{L}_s(\boldsymbol{\theta}^{(t)}; \mathcal{D}_s^{(t-1)})\mathcal{L}_s(\boldsymbol{\theta}; \mathcal{D}_s^{(t)})$ is γ -strongly convex and $(1 + \rho\bar{\ell})$ -jointly smooth.

Proof. At a high level, $(1 + \rho\mathcal{L}_s(\boldsymbol{\theta}^{(t)}); \mathcal{D}_s^{(t-1)})$ acts like a scalar that may scale the strong convexity and joint smoothness coefficient.

Since $\mathcal{L}_s(\boldsymbol{\theta}^{(t)}; \mathcal{D}_s^{(t-1)}) \geq 0$, we know the γ -strong convexity part holds.

Similarly, since $\mathcal{L}_s(\boldsymbol{\theta}^{(t)}; \mathcal{D}_s^{(t-1)}) \leq \bar{\ell}$, we know the $(1 + \rho\bar{\ell})$ -joint smoothness holds. \square

This lemma shows that we can treat $\mathcal{L}_s(\boldsymbol{\theta}^{(t)}; \mathcal{D}_s^{(t-1)})\mathcal{L}_s(\boldsymbol{\theta}; \mathcal{D}_s^{(t)})$ as the fair objective in fair er-weighting mechanisms, where this objective has very similar properties as the fair objectives using the fair penalty mechanism.

Based on the above lemmas, we present a result that bounds the fair-aware loss minimization solution distance from two different input distributions, where [4] and [5] derived similar bounds in the PP cases without fairness penalties.

Lemma D.5. (*Bounding the fair objective minimizers*)

Given fair-aware loss function $\mathcal{L}_{\text{fair}}$ that is γ -strongly convex and $\tilde{\beta}$ -jointly smooth. Then for two distributions $\mathcal{D}, \tilde{\mathcal{D}} \in \Delta(\mathcal{Z})$, denote

$$\boldsymbol{\theta}_{\text{fair}}^* = G(\mathcal{D}; \mathcal{L}_{\text{fair}}) := \arg \min_{\boldsymbol{\theta}} \mathcal{L}_{\text{fair}}(\boldsymbol{\theta}; \mathcal{D}), \quad \tilde{\boldsymbol{\theta}}_{\text{fair}}^* = G(\tilde{\mathcal{D}}; \mathcal{L}_{\text{fair}}) := \arg \min_{\boldsymbol{\theta}} \mathcal{L}_{\text{fair}}(\boldsymbol{\theta}; \tilde{\mathcal{D}}), \quad (19)$$

we have

$$\|\boldsymbol{\theta}_{\text{fair}}^* - \tilde{\boldsymbol{\theta}}_{\text{fair}}^*\|_2 \leq \frac{\tilde{\beta}}{\gamma} \mathcal{W}_1(\mathcal{D}, \tilde{\mathcal{D}}). \quad (20)$$

Proof. Using the strong convexity property and the fact that $G(\mathcal{D}; \mathcal{L}_{\text{fair}})$ is the unique minimizer of $\mathcal{L}_{\text{fair}}(\boldsymbol{\theta}; \mathcal{D})$, we can derive that

$$-\gamma \|G(\mathcal{D}; \mathcal{L}_{\text{fair}}) - G(\tilde{\mathcal{D}}; \mathcal{L}_{\text{fair}})\|_2^2 \geq (G(\mathcal{D}; \mathcal{L}_{\text{fair}}) - G(\tilde{\mathcal{D}}; \mathcal{L}_{\text{fair}}))^\top \nabla_{\boldsymbol{\theta}} \mathcal{L}_{\text{fair}}(\boldsymbol{\theta}; \mathcal{D}). \quad (21)$$

Then for Eqn (8), we observe that

$$(G(\mathcal{D}; \mathcal{L}_{\text{fair}}) - G(\tilde{\mathcal{D}}; \mathcal{L}_{\text{fair}}))^\top \nabla_{\boldsymbol{\theta}} \ell(\boldsymbol{\theta}; Z) \quad (22)$$

is $\|G(\mathcal{D}; \mathcal{L}_{\text{fair}}) - G(\tilde{\mathcal{D}}; \mathcal{L}_{\text{fair}})\|_2 \beta$ -Lipschitz in Z , and

$$(G(\mathcal{D}; \mathcal{L}_{\text{fair}}) - G(\tilde{\mathcal{D}}; \mathcal{L}_{\text{fair}}))^\top \nabla_{\boldsymbol{\theta}} \ell^2(\boldsymbol{\theta}; Z) \quad (23)$$

is $2\bar{\ell} \|G(\mathcal{D}; \mathcal{L}_{\text{fair}}) - G(\tilde{\mathcal{D}}; \mathcal{L}_{\text{fair}})\|_2 \beta$ -Lipschitz in Z , which follows from applying the Cauchy Schwartz inequality and the fact that ℓ is β -jointly smooth.

Then we can derive that

$$(G(\mathcal{D}; \mathcal{L}_{\text{fair}}) - G(\tilde{\mathcal{D}}; \mathcal{L}_{\text{fair}}))^\top \nabla_{\boldsymbol{\theta}} \mathcal{L}_{\text{fair}}(\boldsymbol{\theta}; \mathcal{D}) \geq -(2\rho\bar{\ell} + 1)\beta \mathcal{W}_1(\mathcal{D}, \tilde{\mathcal{D}}), \quad (24)$$

and thus

$$-\gamma \|G(\mathcal{D}; \mathcal{L}_{\text{fair}}) - G(\tilde{\mathcal{D}}; \mathcal{L}_{\text{fair}})\|_2^2 \geq -(2\rho\bar{\ell} + 1)\beta \mathcal{W}_1(\mathcal{D}, \tilde{\mathcal{D}}), \quad (25)$$

we get the proof for Eqn (8), and we can similarly prove this for Eqn (7) and (9). \square

Lemma D.6. (*Bounding the fixed point distribution distance using parameter distance [5]*)

Suppose the transition mapping T is ϵ -jointly sensitive with $\epsilon \in (0, 1)$, then for $\boldsymbol{\theta}_1, \boldsymbol{\theta}_2$ and their corresponding fixed point distributions $\mathcal{D}_1, \mathcal{D}_2$, it holds that

$$\mathcal{W}_1(\mathcal{D}_1, \mathcal{D}_2) \leq \frac{\epsilon}{1 - \epsilon} \|\boldsymbol{\theta}_1 - \boldsymbol{\theta}_2\|_2 \quad (26)$$

Proposition 5.1. (Unique Fair-PS solution) Under Conditions in Lemma 2.4, if $\epsilon(1 + \tilde{\beta}/\gamma) < 1$, then for a given combination of (1) initial distribution $\mathcal{D}^{(0)}$, and (2) fair mechanism with strength ρ , there is a unique Fair-PS solution.

Proof. We define the fixed point transition mapping as

$$\mathbf{T}^{\text{FP}}(\boldsymbol{\theta}; \mathcal{D}) := \mathcal{D}_{\boldsymbol{\theta}} = \mathbf{T}^{\text{FP}}(\boldsymbol{\theta}) \quad (27)$$

the mapping returning the model's fixed point distribution.

Then using the results in Lemma D.2, D.3, D.5, D.4, D.6, we can see that

$$\boldsymbol{\theta}^{(t+1)} = G(\mathbf{T}^{\text{FP}}(\boldsymbol{\theta}^{(t)}); \mathcal{L}_{\text{fair}}) \quad (28)$$

is a contraction mapping when conditions in Lemma 2.4 hold since $\epsilon(1 + \tilde{\beta}/\gamma) < 1$. Therefore, using the Banach fixed-point theorem, we know that there is a unique Fair-PS pair. \square

D.2 Proof of Theorem 5.2

In this part, we provide the convergence of the class of Fair-RRM algorithms in Algorithm 1.

Lemma D.7. ([5]) *Under conditions in Lemma 2.4, given a decision model with parameter $\boldsymbol{\theta}$, denote the parameter returned by Delayed Deployment Scheme as $\hat{\mathcal{D}}_{\boldsymbol{\theta}} := T^{DL}(\boldsymbol{\theta}; \mathcal{D})$ and the fixed point distribution of $\boldsymbol{\theta}$ as $\mathcal{D}_{\boldsymbol{\theta}}$, then*

$$\mathcal{W}_1(\hat{\mathcal{D}}_{\boldsymbol{\theta}}, \mathcal{D}_{\boldsymbol{\theta}}) \leq \frac{\epsilon}{1 - \epsilon} \delta \quad (29)$$

*Proof.*² For a fixed $\boldsymbol{\theta}$ and $\epsilon < 1$, the map $\mathbf{T}(\boldsymbol{\theta}; \cdot)$ is contracting with Lipschitz coefficient ϵ and has a unique fixed point $\mathcal{D}_{\boldsymbol{\theta}}$. Note that $\hat{\mathcal{D}}_{\boldsymbol{\theta}} = \mathbf{T}^{\lceil r \rceil + 1}$, denote $\mathcal{D}^1 = T(\boldsymbol{\theta}; \mathcal{D}^0)$, then

$$\mathcal{W}_1(\hat{\mathcal{D}}_{\boldsymbol{\theta}}, \mathcal{D}_{\boldsymbol{\theta}}) \leq \frac{\epsilon^{\lceil r \rceil}}{1 - \epsilon} \mathcal{W}_1(\mathcal{D}^0, \mathcal{D}^1), \quad (30)$$

then since $r = \log^{-1}(\frac{1}{\epsilon}) \log\left(\frac{\mathcal{W}_1(\mathcal{D}^0, \mathcal{D}^1)}{\delta}\right)$, we have $\epsilon^{\lceil r \rceil} < \epsilon^r = \frac{\delta}{\mathcal{W}_1(\mathcal{D}^0, \mathcal{D}^1)}$, which completes the proof. \square

Theorem 5.2. (Fair-RRM Convergence) Under conditions in Lemma 2.4:

- (i) If $\epsilon(1 + \tilde{\beta}/\gamma) < 1$, Algorithm 1 under the Conventional Schema converges to the Fair-PS pair at a linear rate.
- (ii) If $\epsilon(1 + \tilde{\beta}/\gamma) < 1 - \epsilon$, Algorithm 1 under the k -Delayed Schema converges to the Fair-PS pair at a linear rate for any k .
- (iii) If $\epsilon(1 + \tilde{\beta}/\gamma) < 1$, Algorithm 1 under the Conventional Schema converges to a δ neighborhood of the Fair-PS pair in $O(\log^2 \frac{1}{\delta})$ steps.

proof of (i). We will define a distance metric

$$d_{\text{pair}}((\boldsymbol{\theta}_1, \mathcal{D}_1), (\boldsymbol{\theta}_2, \mathcal{D}_2)) := \mathcal{W}_1(\mathcal{D}_1, \mathcal{D}_2) + \|\boldsymbol{\theta}_1 - \boldsymbol{\theta}_2\|_2. \quad (31)$$

Denote the Fair-RRM mapping as

$$F_{\text{fair}}(\boldsymbol{\theta}, \mathcal{D}) := (G_{\text{fair}}(\boldsymbol{\theta}, \mathcal{D}), \mathbf{T}(\boldsymbol{\theta}; \mathcal{D})) \quad (32)$$

where $G_{\text{fair}}(\boldsymbol{\theta}, \mathcal{D}) := G(\mathbf{T}(\boldsymbol{\theta}; \mathcal{D}); \mathcal{L}_{\text{fair}})$. Then

$$d_{\text{pair}}(F_{\text{fair}}(\boldsymbol{\theta}, \mathcal{D}), F_{\text{fair}}(\boldsymbol{\theta}', \mathcal{D}')) = \mathcal{W}_1(\mathbf{T}(\boldsymbol{\theta}; \mathcal{D}), \mathbf{T}(\boldsymbol{\theta}'; \mathcal{D}')) + \|G_{\text{fair}}(\boldsymbol{\theta}, \mathcal{D}) - G_{\text{fair}}(\boldsymbol{\theta}', \mathcal{D}')\|_2. \quad (33)$$

The ϵ -jointly sensitivity of the transition map \mathbf{T} yields

$$\mathcal{W}_1(\mathbf{T}(\boldsymbol{\theta}; \mathcal{D}), \mathbf{T}(\boldsymbol{\theta}'; \mathcal{D}')) \leq \epsilon \mathcal{W}_1(\mathcal{D}, \mathcal{D}') + \epsilon \|\boldsymbol{\theta} - \boldsymbol{\theta}'\|_2, \quad (34)$$

and using Lemma D.5, we get

$$\|G_{\text{fair}}(\boldsymbol{\theta}, \mathcal{D}) - G_{\text{fair}}(\boldsymbol{\theta}', \mathcal{D}')\|_2 \leq \frac{\tilde{\beta}}{\gamma} \mathcal{W}_1(\mathbf{T}(\boldsymbol{\theta}; \mathcal{D}), \mathbf{T}(\boldsymbol{\theta}'; \mathcal{D}')) \leq \epsilon \frac{\tilde{\beta}}{\gamma} \mathcal{W}_1(\mathcal{D}, \mathcal{D}') + \epsilon \frac{\tilde{\beta}}{\gamma} \|\boldsymbol{\theta} - \boldsymbol{\theta}'\|_2. \quad (35)$$

Combining the above two equations, we get that under conditions in Lemma 2.4, the Fair-RRM mapping is a contraction mapping that has a unique fixed point, where the fixed point satisfies the criteria of being the PS solution.

The proof of this part referenced [5] Theorem 4. \square

²Due to different notations, we present the proof in [5] to help the readers.

proof of (ii). We can derive the sensitivity of $T^k(\mathcal{D}, \boldsymbol{\theta})$ as follows

$$\begin{aligned}
& \mathcal{W}_1(T^k(\mathcal{D}, \boldsymbol{\theta}), T^k(\mathcal{D}', \boldsymbol{\theta}')) \\
& \leq \epsilon \mathcal{W}_1(T^{k-1}(\mathcal{D}, \boldsymbol{\theta}), T^{k-1}(\mathcal{D}', \boldsymbol{\theta}')) + \epsilon \|\boldsymbol{\theta} - \boldsymbol{\theta}'\|_2 \\
& \leq \epsilon^2 \mathcal{W}_1(T^{k-2}(\mathcal{D}, \boldsymbol{\theta}), T^{k-2}(\mathcal{D}', \boldsymbol{\theta}')) + (\epsilon + \epsilon^2) \|\boldsymbol{\theta} - \boldsymbol{\theta}'\|_2 \\
& \leq \dots \\
& \leq \epsilon^k \mathcal{W}_1(\mathcal{D}, \mathcal{D}') + \frac{\epsilon}{1-\epsilon} \|\boldsymbol{\theta} - \boldsymbol{\theta}'\|_2 \\
& < \frac{\epsilon}{1-\epsilon} \mathcal{W}_1(\mathcal{D}, \mathcal{D}') + \frac{\epsilon}{1-\epsilon} \|\boldsymbol{\theta} - \boldsymbol{\theta}'\|_2
\end{aligned} \tag{36}$$

So $T^k(\mathcal{D}, \boldsymbol{\theta})$ is $(\frac{\epsilon}{1-\epsilon})$ -jointly sensitive.

Using the proof of contraction mapping in part (i), we complete the proof of part (ii). \square

proof of (iii). Similar to the above, we denote the parameter returned by the Delayed Deployment Scheme as $\hat{\mathcal{D}}_{\boldsymbol{\theta}} = T^{DL}(\boldsymbol{\theta}; \cdot)$. We have $\boldsymbol{\theta}^{(t+1)} = G(\hat{\mathcal{D}}_{\boldsymbol{\theta}^{(t)}}; \mathcal{L}_{\text{fair}})$.

Recall that $\boldsymbol{\theta}_{\text{fair}}^{\text{PS}} = G(\mathcal{D}_{\text{fair}}^{\text{PS}}; \mathcal{L}_{\text{fair}})$. Then Lemma D.5 indicates that

$$\|\boldsymbol{\theta}^{(t+1)} - \boldsymbol{\theta}_{\text{fair}}^{\text{PS}}\|_2 = \|G(\hat{\mathcal{D}}_{\boldsymbol{\theta}^{(t)}}; \mathcal{L}_{\text{fair}}) - G(\mathcal{D}_{\text{fair}}^{\text{PS}}; \mathcal{L}_{\text{fair}})\|_2 \leq \frac{\tilde{\beta}}{\gamma} \cdot \mathcal{W}_1(\hat{\mathcal{D}}_{\boldsymbol{\theta}^{(t)}}, \mathcal{D}_{\text{fair}}^{\text{PS}}). \tag{37}$$

Using the triangle inequality, we have

$$\mathcal{W}_1(\hat{\mathcal{D}}_{\boldsymbol{\theta}}, \mathcal{D}_{\text{fair}}^{\text{PS}}) \leq \mathcal{W}_1(\hat{\mathcal{D}}_{\boldsymbol{\theta}}, \mathcal{D}_{\boldsymbol{\theta}^{(t)}}) + \mathcal{W}_1(\mathcal{D}_{\boldsymbol{\theta}^{(t)}}, \mathcal{D}_{\text{fair}}^{\text{PS}}), \tag{38}$$

where $\mathcal{D}_{\boldsymbol{\theta}^{(t)}}$ is the fixed point distribution of $\boldsymbol{\theta}^{(t)}$.

We can use Lemma D.7 to get $\mathcal{W}_1(\hat{\mathcal{D}}_{\boldsymbol{\theta}}, \mathcal{D}_{\boldsymbol{\theta}^{(t)}}) \leq \frac{\epsilon \delta}{1-\epsilon}$ and use Lemma D.6 and the sensitivity definition to get $\mathcal{W}_1(\mathcal{D}_{\boldsymbol{\theta}^{(t)}}, \mathcal{D}_{\text{fair}}^{\text{PS}}) \leq \frac{\epsilon}{1-\epsilon} \|\boldsymbol{\theta}^{(t)} - \boldsymbol{\theta}_{\text{fair}}^{\text{PS}}\|_2$.

Therefore,

$$\mathcal{W}_1(\hat{\mathcal{D}}_{\boldsymbol{\theta}}, \mathcal{D}_{\text{fair}}^{\text{PS}}) \leq \frac{\epsilon}{1-\epsilon} (\delta + \|\boldsymbol{\theta}^{(t)} - \boldsymbol{\theta}_{\text{fair}}^{\text{PS}}\|_2). \tag{39}$$

When $\|\boldsymbol{\theta}^{(t)} - \boldsymbol{\theta}_{\text{fair}}^{\text{PS}}\|_2 > \delta$, we have

$$\|\boldsymbol{\theta}^{(t+1)} - \boldsymbol{\theta}_{\text{fair}}^{\text{PS}}\|_2 < \frac{2\epsilon}{1-\epsilon} \frac{\tilde{\beta}}{\gamma} \|\boldsymbol{\theta}^{(t)} - \boldsymbol{\theta}_{\text{fair}}^{\text{PS}}\|_2 \leq \|\boldsymbol{\theta}^{(t)} - \boldsymbol{\theta}_{\text{fair}}^{\text{PS}}\|_2. \tag{40}$$

On the other hand, when $\|\boldsymbol{\theta}^{(t)} - \boldsymbol{\theta}_{\text{fair}}^{\text{PS}}\|_2 \leq \delta$, we have

$$\|\boldsymbol{\theta}^{(t+1)} - \boldsymbol{\theta}_{\text{fair}}^{\text{PS}}\|_2 \leq \frac{2\epsilon}{1-\epsilon} \frac{\tilde{\beta}}{\gamma} \delta \leq \delta \tag{41}$$

Combining the two cases together, we know that for $t \geq \left(1 - \frac{2\epsilon \tilde{\beta}}{\gamma(1-\epsilon)}\right)^{-1} \log\left(\frac{\boldsymbol{\theta}^{(0)} - \boldsymbol{\theta}_{\text{fair}}^{\text{PS}}}{\delta}\right)$, we have

$$\|\boldsymbol{\theta}^{(t)} - \boldsymbol{\theta}_{\text{fair}}^{\text{PS}}\|_2 \leq \left(\frac{2\epsilon}{1-\epsilon} \frac{\tilde{\beta}}{\gamma}\right)^t \delta \leq \delta, \tag{42}$$

which completes the proof for part (iii).

The proof of this part referenced [5] Theorem 8. \square

D.3 Proof of Theorem B.3

In this part, we provide the convergence of the class of fair-RERM algorithms in Algorithm 2.

Theorem B.3 (Fair RERM Convergence) Under conditions in Lemma 2.4, suppose $\exists \alpha > 1, \mu > 0$ such that $\int_{\mathbb{R}^m} e^{\mu|x|^\alpha} Z dx$ is finite $\forall Z \in \Delta(\mathcal{Z})$.

For given a convergence radius $\delta \in (0, 1)$, take $n_t = O\left(\frac{\log(t/p)}{(\epsilon(1+\tilde{\beta}/\gamma)\delta)^m}\right)$ samples at t . If $2\epsilon(1 + \tilde{\beta}/\gamma) < 1$, then with probability $1 - p$, the iterates of fair-RERM are within a radius δ of the Fair-PS pair for $t \geq (1 - 2\epsilon(1 + \tilde{\beta}/\gamma))O(\log(1/\delta))$.

Proof. Given n samples from \mathcal{D} , denote $\hat{\mathcal{D}}^n$ the empirical distribution obtained from them. Denote

$$\hat{G}_{\text{fair}}^n(\boldsymbol{\theta}, \mathcal{D}) := G(\mathbf{T}(\boldsymbol{\theta}; \hat{\mathcal{D}}^n), \quad (43)$$

(recall $G_{\text{fair}}(\boldsymbol{\theta}, \mathcal{D}) := G(\mathbf{T}(\boldsymbol{\theta}; \mathcal{D}); \mathcal{L}_{\text{fair}}$ in Eqn (32)). And also denote the Fair-RERM mapping as

$$\hat{F}_{\text{fair}}(\boldsymbol{\theta}, \mathcal{D}) := (\hat{G}_{\text{fair}}^m(\boldsymbol{\theta}, \mathcal{D}), \mathbf{T}(\boldsymbol{\theta}; \mathcal{D})) \quad (44)$$

By Theorem 2 of [42], since $\exists \alpha > 1, \mu > 0$ such that $\int_{\mathbb{R}^m} e^{\mu|x|^\alpha} Z dx$ is finite $\forall Z \in \Delta(\mathcal{Z})$, then if $n_t = \mathcal{O}\left(\frac{1}{\epsilon(1+\tilde{\beta}/\gamma)^m} \log(t/p)\right)$, where m is the dimension of the sample, we have $\mathcal{W}_1(\mathcal{D}, \hat{\mathcal{D}}^n) \geq \epsilon(1 + \tilde{\beta}/\gamma)\delta$ with probability at most $\frac{6p}{\pi^2 t^2}$.

Therefore,

$$\mathbb{P}(\mathcal{W}_1(\mathcal{D}, \hat{\mathcal{D}}^n) \leq \epsilon(1+\tilde{\beta}/\gamma)\delta, \forall t) = 1 - \sum_{t=1}^{\infty} \mathbb{P}(\mathcal{W}_1(\mathcal{D}, \hat{\mathcal{D}}^{n_t}) > \epsilon(1+\tilde{\beta}/\gamma)\delta) \geq 1 - \sum_{t=1}^{\infty} \frac{6p}{\pi^2 t^2} = 1 - p \quad (45)$$

i.e., with probability at least $1 - \sum_{t=1}^{\infty} 1 - p$ we have that for each time step t , it holds that

$$\mathcal{W}_1(\mathcal{D}, \hat{\mathcal{D}}^n) \leq \epsilon(1 + \tilde{\beta}/\gamma)\delta. \quad (46)$$

Then if $d_{\text{pair}}((\boldsymbol{\theta}, \mathcal{D}), (\boldsymbol{\theta}_{\text{fair}}^{\text{PS}}, \mathcal{D}_{\text{fair}}^{\text{PS}})) \geq \delta$, and Eqn (46) holds, we have

$$\begin{aligned} & d_{\text{pair}}(\hat{F}_{\text{fair}}(\boldsymbol{\theta}, \mathcal{D}), (\boldsymbol{\theta}_{\text{fair}}^{\text{PS}}, \mathcal{D}_{\text{fair}}^{\text{PS}})) \\ &= \mathcal{W}_1(\mathbf{T}(\boldsymbol{\theta}; \mathcal{D}), \mathcal{D}_{\text{fair}}^{\text{PS}}) + \|\hat{G}_{\text{fair}}^n(\boldsymbol{\theta}, \mathcal{D}) - \boldsymbol{\theta}_{\text{fair}}^{\text{PS}}\|_2 \\ &\leq \mathcal{W}_1(\mathbf{T}(\boldsymbol{\theta}; \mathcal{D}), \mathbf{T}(\boldsymbol{\theta}_{\text{fair}}^{\text{PS}}; \mathcal{D}_{\text{fair}}^{\text{PS}})) + \|\hat{G}_{\text{fair}}^n(\boldsymbol{\theta}, \mathcal{D}) - G_{\text{fair}}(\boldsymbol{\theta}, \mathcal{D})\|_2 + \|G_{\text{fair}}(\boldsymbol{\theta}, \mathcal{D}) - G_{\text{fair}}(\boldsymbol{\theta}_{\text{fair}}^{\text{PS}}; \mathcal{D}_{\text{fair}}^{\text{PS}})\|_2 \\ &\leq \epsilon \mathcal{W}_1(\mathcal{D}, \mathcal{D}_{\text{fair}}^{\text{PS}}) + \epsilon \|\boldsymbol{\theta} - \boldsymbol{\theta}_{\text{fair}}^{\text{PS}}\|_2 + \frac{\tilde{\beta}}{\gamma} \mathcal{W}_1(\hat{\mathbf{T}}^n(\boldsymbol{\theta}; \mathcal{D}), \mathbf{T}(\boldsymbol{\theta}; \mathcal{D})) + \frac{\tilde{\beta}}{\gamma} (\mathcal{W}_1(\mathbf{T}(\boldsymbol{\theta}; \mathcal{D}), \mathbf{T}(\boldsymbol{\theta}_{\text{fair}}^{\text{PS}}; \mathcal{D}_{\text{fair}}^{\text{PS}}))) \\ &\leq \epsilon \mathcal{W}_1(\mathcal{D}, \mathcal{D}_{\text{fair}}^{\text{PS}}) + \epsilon \|\boldsymbol{\theta} - \boldsymbol{\theta}_{\text{fair}}^{\text{PS}}\|_2 + \frac{\tilde{\beta}}{\gamma} \epsilon \left(1 + \frac{\tilde{\beta}}{\gamma}\right) \delta + \frac{\tilde{\beta}}{\gamma} (\epsilon \mathcal{W}_1(\mathcal{D}, \mathcal{D}_{\text{fair}}^{\text{PS}}) + \epsilon \|\boldsymbol{\theta} - \boldsymbol{\theta}_{\text{fair}}^{\text{PS}}\|_2) \\ &= \left(1 + \frac{\tilde{\beta}}{\gamma}\right) d_{\text{pair}}((\boldsymbol{\theta}, \mathcal{D}), (\boldsymbol{\theta}_{\text{fair}}^{\text{PS}}, \mathcal{D}_{\text{fair}}^{\text{PS}})) + \epsilon \left(1 + \frac{\tilde{\beta}}{\gamma}\right) \delta \\ &\leq 2\epsilon \left(1 + \frac{\tilde{\beta}}{\gamma}\right) d_{\text{pair}}((\boldsymbol{\theta}, \mathcal{D}), (\boldsymbol{\theta}_{\text{fair}}^{\text{PS}}, \mathcal{D}_{\text{fair}}^{\text{PS}})) \end{aligned} \quad (47)$$

where the third line uses triangle inequality, fourth line uses Lemma D.5, and fifth line uses Eqn (46). In other words, the above shows that if the current pair is more than δ away from the Fair PS solution, then as long as Eqn (46) is true, the Fair RERM mapping is a contraction.

Similarly, if $d_{\text{pair}}((\boldsymbol{\theta}, \mathcal{D}), (\boldsymbol{\theta}_{\text{fair}}^{\text{PS}}, \mathcal{D}_{\text{fair}}^{\text{PS}})) < \delta$, and Eqn (46) holds, we can show that

$$d_{\text{pair}}(\hat{F}_{\text{fair}}(\boldsymbol{\theta}, \mathcal{D}), (\boldsymbol{\theta}_{\text{fair}}^{\text{PS}}, \mathcal{D}_{\text{fair}}^{\text{PS}})) \leq \left(1 + \frac{\tilde{\beta}}{\gamma}\right) d_{\text{pair}}((\boldsymbol{\theta}, \mathcal{D}), (\boldsymbol{\theta}_{\text{fair}}^{\text{PS}}, \mathcal{D}_{\text{fair}}^{\text{PS}})) + \epsilon \left(1 + \frac{\tilde{\beta}}{\gamma}\right) \delta \leq 2\epsilon \left(1 + \frac{\tilde{\beta}}{\gamma}\right) \delta < \delta, \quad (48)$$

which means the pair will stay in the δ radius ball once an iterate goes in the ball.

Then we move on to show when $t \geq \left(1 - 2\epsilon \left(1 + \frac{\tilde{\beta}}{\gamma}\right)\right) \log\left(\frac{d_{\text{pair}}((\boldsymbol{\theta}^{(1)}, \mathcal{D}^{(0)}), (\boldsymbol{\theta}_{\text{fair}}^{\text{PS}}, \mathcal{D}_{\text{fair}}^{\text{PS}}))}{\delta}\right)$ the fair RERM mapping hits the δ radius ball centered at the Fair PS solution. Again, if Eqn (46) holds, then

denote the initial pair as $(\boldsymbol{\theta}^{(1)}, \mathcal{D}^{(0)})$, then we can use similar arguments as above to show that

$$\begin{aligned} d_{\text{pair}}((\boldsymbol{\theta}^{(t+1)}, \mathcal{D}^{(t)}), (\boldsymbol{\theta}_{\text{fair}}^{\text{PS}}, \mathcal{D}_{\text{fair}}^{\text{PS}})) &\leq 2\epsilon \left(1 + \frac{\tilde{\beta}}{\gamma}\right)^t d_{\text{pair}}((\boldsymbol{\theta}^{(1)}, \mathcal{D}^{(0)}), (\boldsymbol{\theta}_{\text{fair}}^{\text{PS}}, \mathcal{D}_{\text{fair}}^{\text{PS}})) \\ &\leq \exp\left(-t \left(1 - 2\epsilon \left(1 + \frac{\tilde{\beta}}{\gamma}\right)\right)\right) d_{\text{pair}}((\boldsymbol{\theta}^{(1)}, \mathcal{D}^{(0)}), (\boldsymbol{\theta}_{\text{fair}}^{\text{PS}}, \mathcal{D}_{\text{fair}}^{\text{PS}})) \\ &\leq \delta. \end{aligned} \quad (49)$$

This completes the proof.

For the k -Delayed RERM, we can follow the proof of part (ii) in Theorem 5.2 that the transition \mathbf{T}^k is $\tilde{\epsilon} := \frac{\epsilon}{1-\epsilon}$ jointly sensitive, and if we replace the ϵ terms with $\tilde{\epsilon}$ and times a k scalar in the number of iterations, we can get the similar result.

The proof of this part referenced Theorem 5 in [5] □

D.4 Proof of the Fairness Guarantee

Discussion of the intricate nature of proving the effectiveness of ρ under the general PP setting.

We first note that it is non-trivial to find out whether fairness at PS solution increases as ρ increases under the general setting where both the group fractions and the group-wise feature-label distributions change. Consider an example where the agents in the minority group are influenced by the majority group, i.e., when their group fraction becomes less than a threshold, their tastes are shaped by the mainstream culture. Then they can change their feature-label distributions to be more similar to the one of the majority group. This will possibly make the loss disparity smaller even when ρ becomes larger. However, in majority of previous work on the retention of recommendation system [2, 12], the group-wise distributions are assumed to be static.

Proof of Theorem 5.4. With Assumption 5.3, we state Lemma D.8.

Lemma D.8 (fairness guarantee at a single step). *At each single step, the following results hold:*

- (i) Given $\mathcal{D}^{(t)}$ fixed (i.e., $p_a^{(t)}, p_b^{(t)}$ stay fixed), increasing ρ in Eqn. (7) leads to lower or equal $\Delta_{\text{fair}, \mathcal{L}}^t(\rho)$;
- (ii) Given the optimization objective fixed (i.e., ρ stays fixed), lower fraction disparity $\Delta_p^{(t)}$ leads to lower or equal $\Delta_{\text{fair}, \mathcal{L}}^t(\rho)$ when the minority group incurs higher loss.

Proof of (i). We prove (i) by contradiction.

Assume $\rho_1 < \rho_2$, and denote the the optimized model parameters as $\theta_{\rho_1}, \theta_{\rho_2}$. Since \mathcal{D}_s does not change over time, we can know the group-wise loss under ρ_1, ρ_2 at both rounds $L_{s, \rho_1}^t = L_{s, \rho_1}^{t-1} = L_{s, \rho_1}$, $L_{s, \rho_2}^t = L_{s, \rho_2}^{t-1} = L_{s, \rho_2}$. Thus, we can interchange the superscript arbitrarily (i.e., if the deployed models are the same, $L_s^t = L_s^{t-1}$). Wlog, assume $L_{a, \rho_1}^t > L_{b, \rho_1}^t$. Then consider all possible scenarios where the loss disparity may be larger:

- $L_{a, \rho_1}^t < L_{a, \rho_2}^t$ and $L_{b, \rho_1}^t < L_{b, \rho_2}^t$: if this holds, then we can just shift θ_{ρ_2} to θ_{ρ_1} to guarantee smaller $L_{a, \rho_2}^t, L_{b, \rho_2}^t$ and therefore smaller $L_{a, \rho_2}^{t-1}, L_{b, \rho_2}^{t-1}$, resulting in a smaller loss specified by Eqn. (7). This produces a contradiction since θ_{ρ_2} is the minimizer;
- $L_{a, \rho_1}^t > L_{a, \rho_2}^t$ and $L_{b, \rho_1}^t > L_{b, \rho_2}^t$: In the same way, we can shift θ_{ρ_1} to θ_{ρ_2} to trivially decrease both $L_{a, \rho_1}^t, L_{b, \rho_1}^t$, violating the condition that θ_{ρ_1} is the minimizer;
- $L_{a, \rho_1}^t < L_{a, \rho_2}^t$ and $L_{b, \rho_1}^t > L_{b, \rho_2}^t$. According to the optimality at ρ_1, ρ_2 , we have:
$$\begin{aligned} p_a \cdot (L_{a, \rho_2}^t - L_{a, \rho_1}^t) + p_b \cdot (L_{b, \rho_2}^t - L_{b, \rho_1}^t) + p_a \cdot \rho_2 \cdot ((L_{a, \rho_2}^t)^2 - (L_{a, \rho_1}^t)^2) + p_b \cdot \rho_2 \cdot ((L_{b, \rho_2}^t)^2 - (L_{b, \rho_1}^t)^2) &< 0 \\ p_a \cdot (L_{a, \rho_2}^t - L_{a, \rho_1}^t) + p_b \cdot (L_{b, \rho_2}^t - L_{b, \rho_1}^t) + p_a \cdot \rho_1 \cdot ((L_{a, \rho_2}^t)^2 - (L_{a, \rho_1}^t)^2) + p_b \cdot \rho_1 \cdot ((L_{b, \rho_2}^t)^2 - (L_{b, \rho_1}^t)^2) &> 0 \end{aligned} \quad (50)$$

Subtract Eqn. (50) from Eqn. (51), we get

$$\begin{aligned} p_a \cdot ((L_{a, \rho_2}^t)^2 - (L_{a, \rho_1}^t)^2) + p_b \cdot ((L_{b, \rho_2}^t)^2 - (L_{b, \rho_1}^t)^2) &< 0 \\ \Leftrightarrow p_a \cdot (L_{a, \rho_2}^t + L_{a, \rho_1}^t) \cdot (L_{a, \rho_2}^t - L_{a, \rho_1}^t) + p_b \cdot (L_{b, \rho_2}^t + L_{b, \rho_1}^t) \cdot (L_{b, \rho_2}^t - L_{b, \rho_1}^t) &< 0 \end{aligned} \quad (52)$$

From Eqn. (52) and Eqn. (51), we can immediately get:

$$p_a \cdot (L_{a,\rho_2}^t - L_{a,\rho_1}^t) + p_b \cdot (L_{b,\rho_2}^t - L_{b,\rho_1}^t) > 0 \quad (53)$$

Otherwise Eqn. (51) would be smaller than 0. We have by assumption $L_{a,\rho_2}^t > L_{a,\rho_1}^t > L_{b,\rho_1}^t > L_{b,\rho_2}^t$. Then $L_{a,\rho_1}^t + L_{a,\rho_2}^t > L_{b,\rho_1}^t + L_{b,\rho_2}^t$. Next, noticing that $L_{b,\rho_2}^t - L_{b,\rho_1}^t < 0$ and $L_{a,\rho_2}^t - L_{a,\rho_1}^t > 0$, then if we divide $L_{a,\rho_1}^t + L_{a,\rho_2}^t$ at both sides of Eqn. (52), then we will get:

$$p_a \cdot (L_{a,\rho_2}^t - L_{a,\rho_1}^t) + p_b \cdot \frac{(L_{b,\rho_2}^t + L_{b,\rho_1}^t)}{(L_{a,\rho_2}^t + L_{a,\rho_1}^t)} \cdot (L_{b,\rho_2}^t - L_{b,\rho_1}^t) < 0 \quad (54)$$

However, the LHS of Eqn. (54) is larger than the LHS of Eqn. (53), while the LHS requires the opposite, producing a contradiction. Finally, note that it is impossible to let loss of one group stays fixed while the other one changes where we can easily prove with similar contradictions.

Since all the above scenarios do not hold, we have proved (i). Moreover, if for any $\rho_2 > \rho_1$, the loss disparities are equal, it means that both groups achieve minimal loss with a same θ^* , which is very uncommon considering the difference of demographic groups. Thus, increasing ρ commonly leads to lower loss disparity $\Delta_{\mathcal{L}}^{(t)}$. \square

proof of (ii). Next, we prove (ii) similarly. Denote the optimized group-wise loss under the two group fractions as $L_s^{(t)}$ and $L_{s'}^{(t)}$. Wlog, assume $L_a^{(t)} > L_b^{(t)}$. We will have the following equations:

$$p_{a'}^{(t)} \cdot (L_{a'}^{(t)} - L_a^{(t)}) + p_{b'}^{(t)} \cdot (L_{b'}^{(t)} - L_b^{(t)}) < 0 \quad (55)$$

$$p_a^{(t)} \cdot (L_{a'}^{(t)} - L_a^{(t)}) + p_b^{(t)} \cdot (L_{b'}^{(t)} - L_b^{(t)}) > 0 \quad (56)$$

To prove by contradiction, we need to consider the situations where the group fraction discrepancy becomes smaller. This can be either $p_a^{(t)} < p_b^{(t)}$, $p_{a'}^{(t)} > p_a^{(t)}$ or $p_a^{(t)} > p_b^{(t)}$, $p_{a'}^{(t)} < p_a^{(t)}$. Then consider all possible scenarios where the loss disparity may be larger:

- $L_a^{(t)} < L_{a'}^{(t)}$ and $L_b^{(t)} < L_{b'}^{(t)}$: Eqn. (55) does not hold;
- $L_a^{(t)} > L_{a'}^{(t)}$ and $L_b^{(t)} > L_{b'}^{(t)}$: Eqn. (56) does not hold;
- $L_a^{(t)} < L_{a'}^{(t)}$ and $L_b^{(t)} > L_{b'}^{(t)}$: Subtract Eqn. (55) from Eqn. (56), we can get:

$$(p_a^{(t)} - p_{a'}^{(t)}) \cdot (L_{a'}^{(t)} - L_a^{(t)}) + (p_b^{(t)} - p_{b'}^{(t)}) \cdot (L_{b'}^{(t)} - L_b^{(t)}) > 0 \quad (57)$$

Noticing that $p_a^{(t)} - p_{a'}^{(t)} = -(p_b^{(t)} - p_{b'}^{(t)})$, then only when $p_a^{(t)} - p_{a'}^{(t)} > 0$ we can make the above inequality holds. According to the situations where the group fraction discrepancy becomes smaller, we know $p_a^{(t)} > p_b^{(t)}$ must hold and a is the majority group. However, this contradicts the initial condition $L_a^{(t)} > L_b^{(t)}$, i.e, the majority group should not have higher group-wise loss.

Finally, it is easy to see the cases where losses stay fixed cannot satisfy Eqn. (55) and Eqn. (56) simultaneously. Thus, we prove (ii). \square

With Lemma D.8, we can easily prove Thm. 5.4. What we need to prove is $\Delta_{\text{fair},\mathcal{L}}^{\text{PS}}(\rho_1) \geq \Delta_{\text{fair},\mathcal{L}}^{\text{PS}}(\rho_2)$. Now we know at t , higher ρ results in lower or equal $\Delta_{\text{fair},\mathcal{L}}^t(\rho)$ ((i) of Lemma D.8). Then the lower or equal $\Delta_{\text{fair},\mathcal{L}}^t(\rho)$ results in lower group fraction disparity at $t + 1$ (Assumption 5.3), and further causes lower loss disparity at $t + 1$ ((ii) of Lemma D.8). This enables a forward induction to prove that $\Delta_{\text{fair},\mathcal{L}}^t(\rho)$ is non-decreasing with ρ at each time step to infinity, which completes the whole proof of Thm. 5.4.

D.5 Discussion on Performative Optimal (PO) Solutions

The PO solution is defined as

$$\boldsymbol{\theta}^{\text{PO}} := \mathbb{E}_{Z \sim \mathcal{D}_\theta} \ell(\boldsymbol{\theta}; Z), \quad (58)$$

\mathcal{D}_θ is the fixed point distribution.

At a high level, the PO solution and the approximation between PS and PO solution largely follows the analysis in [4, 5], where Theorem 6 in [5] states that if conditions in Lemma 2.4 and $\ell(\cdot; \cdot)$ is L_z -Lipschitz in the second argument, then the PS and Po solution satisfies

$$\|\boldsymbol{\theta}^{\text{PO}} - \boldsymbol{\theta}^{\text{PS}}\|_2 \leq \frac{2L_z \epsilon}{\gamma(1 - \epsilon)}.$$

We note that the corresponding proof and the bound both only depend on the strong convexity coefficient γ and sensitivity coefficient ϵ , where the fair objective and the original objective have the same values, but the fair objective did change the Lipschitz coefficient to $\tilde{L}_z := (1 + \rho \bar{\ell}^2)L_z$ and $\tilde{L}_z := (1 + \rho \bar{\ell})L_z$ when using fair penalty and fair reweighting mechanisms, respectively. Therefore, as long as we replace L_z with the corresponding new value \tilde{L}_z , we can use the same proof steps to show that

$$\|\boldsymbol{\theta}_{\text{fair}}^{\text{PO}} - \boldsymbol{\theta}_{\text{fair}}^{\text{PS}}\|_2 \leq \frac{2\tilde{L}_z \epsilon}{\gamma(1 - \epsilon)},$$

where

$$\boldsymbol{\theta}_{\text{fair}}^{\text{PO}} := \arg \min_{\boldsymbol{\theta}} \mathcal{L}_{\text{fair}}(\boldsymbol{\theta}; \mathcal{D}_\theta)$$

But as we show previously, the fairness metrics are only stable and meaningful in PP when measured at the PS and Fair-PS solutions, so there isn't much practical value in finding the FPO solution.